COMMISSARIAT A L'ENERGIE ATOMIQUE

CENTRE D'ETUDES NUCLEAIRES DE SACLAY
Service de Documentation
F91191 GIF SUR YVETTE CEDEX

CEA-CONF - - 8329

L7

USE OF PSEUDOPOTENTIALS IN ATOM-ATOM (OR MOLECULE) COLLISIONS

JEAN PASCALE

SERVICE DE PHYSIQUE DES ATOMES
ET DES SURFACES
CENTRE D'ÉTUDES NUCLÉAIRES DE SACLAY
91191 GIF-SUR-YVETTE CEDEX, FRANCE

Communication présentée à : 12. Summer school on quantum optics
Frombork (Poland)
2-8 Sep 1985

TABLE OF CONTENTS

USE OF PSEUDOPOTENTIALS IN ATOM-ATOM (OR MOLECULE) COLLISIONS

Jean Pascale

Service de Physique des Atomes et des Surfaces, Centre d'Etudes Nucléaires de Saclay, 91191 Gif-sur-Yvette Cedex, France

1. Introduction

Knowledge of interactions betweens ions, atoms or molecules is fundamental for interpretating or predicting collisional processes which may occur under various circumstances. The aim of this paper is to demonstrate the usefulness of using semiempirical effective interactions (more particularly, emphasis will be put on the pseudopotential approach) in the study of atom-atom (or molecule) collisions. Therefore, we will not review in this paper the numerous theoretical works devoted to various atom-atom (ion or molecule) systems and using a semiempirical effective interaction approach. Instead, we would like to show that if the semiempirical effective interactions are carefully defined, their use in molecular-structure calculations and in collision problems can give quite accurate results. These can be of comparable or even higher quality than those obtained from more sophisticated approaches. We will limit our examples to one-electron systems, while extension to more than one valence electron does not present any particular difficulty in principle. The alkali-metal (M) -atom - rare gas systems, which may be reduced to interactions between a one valence electron only and two closed-shell cores are certainly the most appropriate systems to be studied using an effective interaction approach. Moreover, these systems are easy to handle in laboratories, and so a large amount of experimental data has been produced up to now, leading to numerous confrontations between experiment and theory. In this paper, we will consider the M-atom-He systems as a first example. For these systems, recent molecular-structure calculations have been carried

out using an l-dependent semiempirical pseudopotential approach (Pascale, 1983a) and they have been tested against numerous experimental data in extensive calculations of cross sections for intra- and -inter-doublet transitions in the M-atom in collisions with He (Pascale, 1983 b, c, and to be published ; Kimura and Pascale, 1985). Our second example will concern the M-H_2 systems, for which semiempirical pseudopotential molecular-structure calculations have been performed very recently (Rossi and Pascale, 1985) using a one-electron two-center model (in which the molecular nature of H_2 is accounted for). The results of these calculations are quite encouraging and we foresee the use of the pseudopotential approach in future studies of some reactive scattering processes.

2. Pseudopotential molecular-structure calculations

A - Generalities

Let us consider the interaction between two atoms or ions. Generally, one has to solve the Schrödinger equation describing the whole system within the Born-Oppenheimer (BO) approximation, in which the nuclear and electronic wave functions are separable. Therefore, one needs to solve the electronic Schrödinger equation,

$$H_{el}\,\psi_{el} = E_{el}(R)\,\psi_{el}\,, \qquad (1)$$

for any fixed distance R between the two nuclei, in order to obtain the electronic energy $E_{el}(R)$. In Eq. (1), H_{el} is the full electronic Hamiltonian which contains all the one-electron kinetic-energy operators and all the Coulombic interactions involving the electrons. Then, the adiabatic potential energy E(R) of the system for a given state is defined as the sum of $E_{el}(R)$ and of the Coulombic repulsion between the nuclei.

A.1 - Full electron *ab initio* methods

For solving Eq. (1) by *ab initio* methods one makes no approximation, at any stage of the calculations, which would require either the use of some experimental data or other input not determined from fundamental principles. Generally, in order to solve Eq. (1), a variational procedure is used. It consists of defining an approximate electronic wave function ψ_a depending on several parameters, and in varying these parameters to minimize the expectation value

$$\langle \psi_a | H_{el} | \psi_a \rangle = E_a \ , \qquad (2)$$

where E_a is the approximate electronic energy. Obviously, the accuracy of such calculations will depend upon the flexibility of ψ_a. Usually, ψ_a may be obtained within the Hartree-Fock self-consistent-field (HF-SCF) approximation, in which each electron moves in the average potential due to the other electrons of the system. Then correlations between the electrons may be accounted for by configuration interaction (CI) calculations (some aspects of these *ab initio* methods are discussed by W.E. Baylis elsewhere in this volume). To illustrate the complexity of such calculations, when a high accuracy of the results is expected, let us consider the all-electron CI calculations of Saxon et al. (1977) for the NaAr system. In these calculations, where the eleven electrons of Na and the eighten electrons of Ar are considered, ψ_a was expanded in terms of orthonormal configuration state functions (CSF). Each CSF was written as a linear combination of slater determinants (SD). And each SD was built from an orthonormal basis set of one-electron wave functions expanded in terms of Slater-type orbitals (STO), including STO's with large values of the orbital quantum number l to account correctly for dispersion forces. To obtain the adiabatic potential energies of the $X^2\Sigma^+$, $B^2\Sigma^+$ and $A^2\Pi$ states, 2568 (for the $^2\Sigma^+$ states) or 4235 (for the $^2\Pi$ state) CSF's were included in the calculations. However, in order to reduce the computation time, only interatomic valence correlation energies were considered in these calculations. The results showed large deviations of the CI calculations from the SCF calculations and improved the agreement between experiment (York et al., 1975) and previous semiempirical pseudopotential calcula-

tions (Baylis, 1969 ; Pascale and Vandeplanque, 1974). However, the results showed also some deficiencies of the CI calculations, due mainly to the neglect of intra-atomic valence correlation energies.

Because the computer time and computer storage increase rapidly as the number of basis functions increases, the need of introducing some simplifications in the treatment of large systems becomes manifest. Simplifications in the calculations, without loss of accuracy, is the purpose of using effective interactions.

A.2 - *Ab initio* effective potential methods

The basic idea of these methods is that only the outermost valence electrons of the atoms (or ions) constituting the molecular system are important in determining the chemical bonding. Thus, the full-electron calculations are simplified by separating the electrons of the system into valence and core electrons. An effective potential is defined to describe the interaction between a valence electron and the core electrons. Then, in CI calculations the core electrons are "frozen" and only the correlations between the valence electrons are considered. There has been a quite large number of reviews on *ab initio* effective interaction methods (see for example, Weeks et al., 1969 ; Bardsley, 1974 ; Kahn et al., 1976 ; Barthelat et al., 1977 ; Dixon and Robertson, 1978) to which we refer the reader for details. Here, we just survey the effective interaction approach by considering again the example of the NaAr system studied by Laskowsky et al. (1981). In this approach, Na is considered as a core A and one valence electron, and Ar as a core B and eight valence electrons. The electronic Hamiltonian of the system is written as,

$$H_{el} = \sum_{i=1}^{N} \left[-\frac{1}{2}\nabla_i^2 + \sum_x \left(-\frac{Z_x}{r_{ix}} + v_{ix} \right) + \sum_{j>i} \frac{1}{r_{ij}} \right] \qquad (3)$$

where N = 9 and Z_x is the nuclear charge of the core x (A or B). The problem is then to determine an effective potential v_{ix} which describes the interaction between a valence electron e_i^- and the core x. Defining the one-electron Hamiltonian as :

$$h_{ix} = -\frac{1}{2}\nabla_i^2 - \frac{Z_x}{r_{ix}} + v_{ix} \,, \tag{4}$$

the effective potential v_{ix} is such that the valence electron wave function φ_{ix} satifies the Schrödinger equation :

$$h_{ix}\varphi_{ix} = \varepsilon_{ix}\varphi_{ix} \tag{5}$$

where ε_{ix} is the valence electron energy. Provided that φ_{ix} is orthogonal to all the core orbitals, in order to satisfy the Pauli principle, v_{ix} can be defined as a non-local operator in terms of both the valence and core orbitals (note that the orthogonality of φ_{ix} to all the core orbitals implies that the radial part of φ_{ix} oscillates in the core region). However, such a definition of v_{ix} is not very useful for molecular-structure calculations because all the core orbitals have then to be considered in the basis function set. In the pseudopotential approach, first one restricts the non-locality of v_{ix} to the angular momentum dependence, defining

$$v_{ix} = \sum_l v_{ix}^{(l)}(r_{ix})\mathcal{P}_l^x \,, \tag{6}$$

where $\mathcal{P}_l^x$ is an l-projector on the center x. Second, for each l-symmetry, the local potential $v_{ix}^{(l)}(r_{ix})$ is defined such that the radial pseudo-wave function of the valence electron in its lowest state has no node, but is identical to the true valence wave function at large distance r_{ix}. With such a definition v_{ix}, the orthogonality constraints of φ_{ix} to all the core orbitals are implicitely satisfied, and the core orbitals can be safely ignored in the molecular-structure calculations. In the *ab initio* pseudopotential-CI calculations of Lakowsky et al. (1981) for NaAr, all the correlations among the nine valence electrons were considered. However, because their basis set of Gaussian functions did not include large values of l, their calculations failed to predict correctly the dispersion energies in spite of the large computational effort which was required (several thousands of CSF's were used). These calculations, as well as those of Saxon et al. (1977), illustrate clearly the considerable amount of work needed in CI-*ab initio* methods to predict correctly the dispersion

energies. To overcome these difficulties, an *ab initio* method has been proposed recently by M. Hliwa et al. (1985) for the calculation of dispersion energies. This method, prompted by the perturbative approach of Bottcher and Dalgarno (1974), does not require the definition of a cut-off radius as in the semiempirical model potential or pseudopotential approaches described below ; but it is limited to dipolar terms. While the method seems promising, its application to NaAr in particular is not fully convincing (due to an insufficient knowledge of the core-core interaction, a scaling of the theoretical results to an experimental ground-state potential curve was necessary for improving the agreement between experiment and theory).

A.3 - Semiempirical effective potential methods (model potential (MP) and pseudopotential (PP) approaches)

In these methods the effective potentials discussed above are determined by modeling fully or partly the interactions in order to reproduce accurately some experimental data. In that sense these methods are semiempirical.

In order to illustrate these approaches, let us consider again the example of an alkali-metal (M)-atom-rare gas system. Because both the M-ion and the rare gas have closed-shell structures, the problem of determining the interaction between the M-atom and the rare gas is reduced to a three-body problem (namely a core A representing the M-ion, the valence electron e^-, and a core B representing the rare gas, as in Fig. 1 , in which the two-body interactions are described by effective potentials. An effective Hamiltonian describing the three-body system may be written as

$$H_{eff} = H_{el} + V_{AB}(R) \quad , \tag{7}$$

with

$$H_{el} = -\frac{1}{2}\nabla^2_{\vec{r}_x} + V_A + V_B + V_{CT}(\vec{r}_x, \vec{R}) \quad . \tag{8}$$

V_x, $x \equiv A$ or B and V_{AB}. are effective potentials describing, respectively

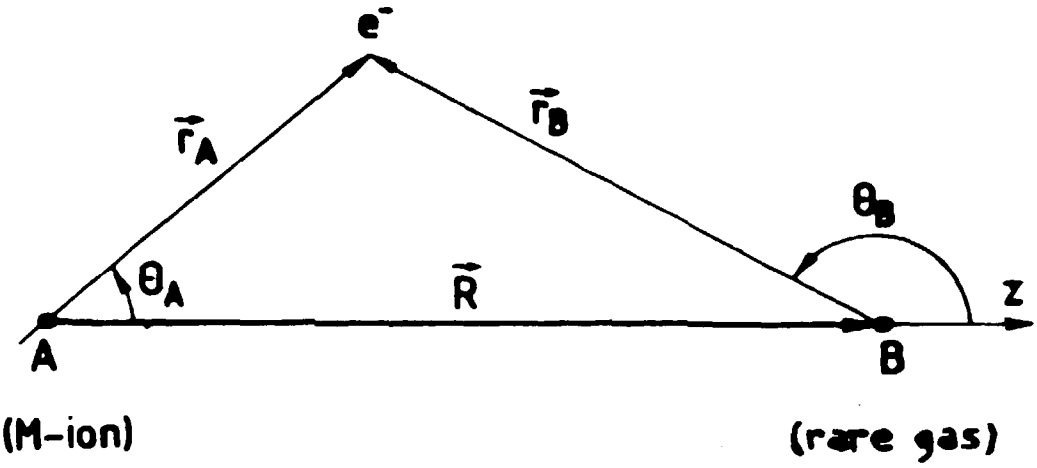

Fig. 1 - The three-body model describing the alkali-metal-atom-rare gas interaction.

the e^--x and core-core interactions. $V_{CT}(\vec{r}_x, \vec{R})$ is a term (the so-called cross term defined later on) which must be included in the calculations in order to have the correct behavior of the adiabatic potential energies at large internuclear distances R. This term depends both of the position vector $\vec{r}_x$ of e^- with respect to the core x, and of the position vector $\vec{R}$ of B with respect to A (see Fig. 1). As before, the electronic energies $E_{el}(R)$ are obtained by solving the one-electron Schrödinger equation (1) corresponding to the effective electronic Hamiltonian (Eq. (8)) and the adiabatic potential energies are then :

$$E(R) = E_{el}(R) + V_{AB}(R) \quad . \tag{9}$$

The determination of V_{AB} may cause a real problem in some cases. Usually, V_{AB} may be modeled to fit some reliable experimental scattering data, when available.

Let us discuss here the effective potential V_x describing the e^--x interaction. Its determination has become rather standard and depends only on the approach chosen : model potential or pseudopotential. In general, V_x is separated into a short-range part and a long-range part :

$$V_x = V_x^{SR} + V_x^{LR}(r_x) \tag{10}$$

The long-range part may be expressed as a local potential $V_x^{LR}(r_x)$, a sum of polarization terms and of the Coulombic interaction between e^- ans the net charge of the core x. The polarization terms are relatively well-known at large values of r_x (see, for example, Buckingham, 1967 ; Peach, 1983), but their extension to small values of r_x require to the introduction of analytic cut-off functions which are rather arbitrarily defined. The short-range part, V_x^{SR}, is now defined such that the valence electron wave function satisfies the Schrödinger equation,

$$\left[-\frac{1}{2} \nabla^2_{\vec{r}_x} + V_x^{SR} + V_x^{LR}(r_x) \right] \varphi(\vec{r}_x) = \varepsilon \varphi(\vec{r}_x) \tag{11}$$

ε is the valence electron energy which can be negative (bound state) or positive (continuum state). When x is an M-ion, V_x^{SR} is usually modeled to reproduce correctly the nl-energy levels of the M-atom ; when x is a rare gas, V_x is modeled to reproduce low-energy e^--x elastic scattering experimental data (usually, the lowest l-wave phase shifts and the scattering length). Now, the distinction between pseudopotential (PP) and model potential (MP) approaches comes essentially from the definition of V_x^{SR}, or more exactly from the conditions imposed on $\varphi(\vec{r}_x)$. To be more specific let us consider first the case where x is an M-ion ($x \equiv A$).

If one puts $V_A^{SR} = 0$ and $\varepsilon = \varepsilon_{nl}$, the experimental energy of a given nl level of the M-atom, and integrates the radial Schrödinger equation corresponding to Eq. (11) inward from infinity :

$$\left[-\frac{1}{2} \frac{d^2}{dr_A^2} - \frac{l\,(l+1)}{2\,r_A^2} + V_A^{LR}(r_A) \right] R_{nl}(r_A) = \varepsilon_{nl}\, R_{nl}(r_A) \ , \tag{12}$$

one finds the following results : $R_{nl}(r_A)$ behaves correctly at large r_A-values, but may oscillate for $r_A \to 0$ because $V_A^{LR}(r_A)$ is attractive and the effective potential $\frac{l(l+1)}{2r_A^2} + V_A^{LR}(r_A)$ may support several bound states for the lowest values of l. In the PP approach, one defines V_A^{SR} in terms

of projectors onto the angular momentum l as discussed in Sec A.1,

$$V_{Al}^{SR} = \sum_{l=o}^{\infty} V_{Al}^{SR}(r_A)\mathcal{P}_l^A \qquad (13)$$

Then, for each l-symmetry, the local potential $V_{Al}^{SR}(r_A)$ is introduced in Eq. (12) and modeled so that the pseudo-radial wave function $R_{nl}^{PP}(r_A)$ has no node for the lowest nl level. Let l_{max}-1 be the largest value of l corresponding to a real bound state of the core. Then, one finds that for $l < l_{max}$ $V_{Al}^{SR}(r_A)$ has to be repulsive to satisfy the Pauli principle. For $l \geq l_{max}$, $V_{Al}^{SR}(r_A)$ has to be attractive to take into account the incomplete screening of the nucleus by the core electrons for small r_x-values. Usually it is enough to take $V_{Al}^{SR}(r_A) = V_{Al_{max}}^{SR}(r_A)$ for $l > l_{max}$, so that the summation in Eq. (13) is limited only to a few terms. In the MP approach, $V_{Al}^{SR}(r_A)$ is introduced in Eq. (12) and modeled so that the model potential-radial wave function $R_{nl}^{MP}(r_A)$ has the correct number of nodes (n-l-1 nodes). Then virtual bound states are predicted, which may correspond closely to the real bound states of the core. Usually, a local potential (in the sense that it does not depend on l) can be found, which allows one to fit closely the experimental energy levels ε_{nl} of the M-atom. The non-locality of the e^--A interaction, as discussed in Sec. A.2, is then reflected by the conditions that the valence electron wave function $\varphi^{MP}(\vec{r}_A)$ must be orthogonal to the wave functions of the virtual bound states.

In the case where x is a rare gas atom (X ≡ B) the definition of V_B^{SR}, in the PP or MP approach, is equivalent to above by considering the Levinson's theorem (see, for example, de Alfaro and Regge, 1965) for the e^--x elastic scattering : the number n_l of real bound states of the core x corresponds to an l-wave phase shift $\eta_l(E)$ such that

$$\eta_l(E = 0) = n_l \pi , \qquad (14)$$

where E is the incident electron energy. Therefore, when solving the radial Schrödinger equation similar to Eq. (12) but with ε_{nl} replaced by E, in order to determine $\eta_l(E)$, a local potential is introduced in a manner

equivalent to above. In the PP approach an l-dependent short-range potential $V_{Bl}^{SR}(r_B)$ is modeled so that $\eta_l^{PP}(E)$ fits the experimental l-wave phase shift $\eta_l^{exp}(E)$ (modulo π) at low energies, and satisfies

$$\eta_l^{PP}(E = 0) = 0 \qquad (15)$$

For $l < l_{max}$ (where l_{max} is defined above), $V_{Bl}^{SR}(r_B)$ is repulsive to simulate the Pauli principle, and for $l \geq l_{max}$ it is attractive and, $V_{Bl}^{SR}(r_B) = V_{Bl_{max}}^{SR}(r_B)$. In the MP approach, a local short range potential is modeled such that $\eta_l^{MP}(E)$ fits $\eta_l^{exp}(E)$ at low energies, and satisfies Eq. (14) ; moreover, $\varphi^{MP}(\vec{r}_B)$ must satisfy the requirement that it is orthogonal to the wave functions of the virtual bound states of the same symmetry predicted by the effective potential V_B. An attractive potential $V_B^{SR}(r_B)$, independent of l, is generally determined, which should predict virtual bound states as close as possible of the real ones. However, this condition is difficult to realize since V_B does not contain any Coulombic term, and therefore makes the position of the virtual bound states very sensitive to $V_B^{SR}(r_B)$. Two procedures have been proposed : $V_B^{SR}(r_B)$ may be modeled by fitting $-\eta_l^{exp}(E)$ at low energies, with the constraint that $\varphi^{MP}(\vec{r}_B)$ is orthogonal to HF core orbitals of the same symmetry when solving the radial Schrödinger equation (see, for example, Philippe et al., 1979) ; or $V_B^{SR}(r_B)$ may be modeled by fitting $\eta_l^{exp}(E)$ over a larger domain of energies than above (G. Peach, 1982).

Given the interactions V_x and the cross term $V_{CT}(\vec{r}_x, \vec{R})$ defining the electronic Hamiltonian (Eq. 8), the electronic energies $E_{el}(R)$ and the electronic wave functions $\psi_{el}(\vec{r},\vec{R})$ are usually obtained by solving the one-electron Schrödinger equation (Eq. 1) with standard variational procedures. But, whereas in the PP approach $\psi_{el}(\vec{r},\vec{R})$ has only to tbe expanded over a basis set of valence orbitals centered on the M-atom the MP approach requires that the basis set includes also orbitals describing the virtual bound states of the M-ion and of the rare gas atom. Therefore, the PP approach appears to be more efficient for molecular-structure calculations over the MP approach when the number of core electrons increases. In par-

ticular, for two-valence electrons systems the MP approach may give rise to instabilities of $E_{el}(R)$ at small R (see, Mo et al., 1985) due to the presence of virtual bound states, while the PP approach avoids these problems in principle.

In the following sections we present recent applications of the PP approach to molecular-structure calculations of M-atom-He (Pascale, 1983a) and M-atom-H_2 systems (Rossi and Pascale, 1985).

B - Recent applications of the PP approach

B.1 - M-atom-He systems. The interaction between the M-atom and He is described by the above three-body model (see Fig. 1).

B.1.a - The interactions. The effective interaction V_x between e^- and the core x is separated as in Eq. (10) into a short-range part V_x^{SR} and a long-range par V_x^{LR}. For V_x^{SR} we use an l-dependent pseudopotential (see Eq. 13), where the local potential $V_{xl}(r_x)$ is of Gaussian-type :

$$V_{xl}(r_x) = C_{xl} \exp(- D_{xl} r_x^2) \tag{16}$$

and C_{xl} and D_{xl} are parameters. For V_x^{LR}, we use a local potential,

$$V_x^{LR}(r_x) = - \frac{Z_x}{r_x} - \frac{1}{2} \frac{\alpha_{d_x}}{(r_x^2 + d_x^2)^2} - \frac{1}{2} \frac{\alpha' q_x}{(r_x^2 + d_x^2)^3} \tag{17}$$

Z_x is the net charge of the core ; α_{d_x} is the experimental static dipole polarizability, and

$$\alpha'_{q_x} = \alpha_{q_x} - 6 \beta_x + 2 \alpha_{d_x} d_x^2 , \tag{18}$$

where α_{q_x} is the experimental static quadrupole polarizability ; β_x is a dynamical correction to the static dipole polarizability and d_x is a cut-off radius to be adjusted. In the case of the M-ion, β_A was considered as a

parameter. Then the parameters of the effective interactions were determined by fitting some experimental data. In the case of the e^--M-ion interaction, the parameters were obtained by reproducing the experimental energies levels of the M-atom (we have used the values determined by Bardsley, 1974). For the e^--He interaction, the parameters were obtained by fitting experimental l-wave phase shifts (s, p, and d waves) of Williams (1979), as well as the value of the scattering length, namely 1.18 au (atomic units) determined by O'Malley et al. (1979).

The core-core interaction $V_{AB}(R)$ was taken as

$$V_{AB}(R) = V_{AB}^{SR}(R) - \frac{1}{2} \frac{\alpha_{d_B}}{(R^2 + d_B^2)^2} - \frac{1}{2} \frac{\alpha''_{q_B}}{(R^2 + d_B^2)^3} \qquad (19)$$

where $\alpha''_{q_B} = \alpha_{q_B} + 2\,\alpha_{d_B}\, d_B^2$, and the short-range part of the potential was modeled as

$$V_{AB}^{SR}(R) = a \exp(-b R) \qquad (20)$$

Then the parameters a and b were adjusted by fitting the experimental $X^1\Sigma^+$ potential curves of the M-ion-He systems (Inouye et al., 1979) obtained from elastic scattering experiment in the 0.5-4 keV energy range. We refer to Pascale (1983a) for a tabulation of the various parameters used in the calculations.

Finally, in order to define fully the one-electron Hamiltonian, we need to determine the cross-term $V_{CT}(\vec{r}_x,\vec{R})$ which results from the polarization of He by both e^- and the M-ion. This term is important to obtain the correct behavior of the adiabatic potentials at large internuclear distances :

$$E_i(R) - E_i(\infty) = -\frac{\alpha_{d_B}}{R^6} \langle r_A^2 \,(1 + P_2(\vec{r}_A)) \rangle_i + \frac{3\beta_B}{R^6} \qquad (21)$$

where $\langle\ \rangle_i$ denotes the average value with respect to the wave function of the M-atom in the state i. The expression of $V_{CT}(\vec{r}_x,\vec{R})$ is well-known asymptotically (see, for example, Peach, 1983). For any position $(\vec{r}_x,\vec{R})$ one may use :

$$V'_{CT}(\vec{r}_B,\vec{R}) = \frac{\alpha d_B \xi_B}{(R^2 + d_B^2)(r_B^2 + d_B^2)} + \frac{1}{2}\frac{\alpha'' q_B (3\xi_B^2 - 1)}{(R^2 + d_B^2)^{3/2}(r_B^2 + d_B^2)^{3/2}} \qquad (22)$$

whith is consistent with the polarization terms used in Eqs. (17) and (19), where $\xi_B = \hat{r}_B.\hat{R}$ ($\hat{r}_B = \vec{r}_B/r_B$). But since this expression is only valid when the electronic charge densities of the two atoms do not overlap, it was proposed (Pascale, 1983a) to use

$$V_{CT}(\vec{r}_B,\vec{R}) = V'_{CT}(\vec{r}_B,\vec{R})\, f_c\left(\frac{R}{r_A}\right) \qquad (23)$$

where the additional cut-off function in R/r_A forces V_{CT} smoothly to zero for $r_A \geq R$.

B.1.b - Molecular-structure calculations. The electronic wave function $\psi_e(\vec{r}_A,R)$ was expanded over a large basis set of STO for the M-atom, where $\vec{R}$ is chosen as the quantization axis. The non-linear parameters of the STO's were optimized in order to reproduce accurately the ionization energies of the excited levels up to the first nG level (with an accuracy generally better than $2.5\ 10^{-4}$ au) ; they were kept constant for all R-values. The electronic energies (up to the first nG level of the M atom) were obtained from the diagonalization of the electronic hamiltonian (Eq. (8)) for each value of the projection M_L of the total orbital momentum $\vec{L}$ (equal to that of the valence electron, in the present case). The calculations were performed for all the M-atom-He system in the range R = 2 - 50 a.u.

B.1.c - Results and discussion. To illustrate the accuracy of the PP calculations (J. Pascale, 1983a), let us consider the case of the NaHe and CsHe systems. Fig. 2 shows the comparisons of the PP calculations with the $X^2\Sigma$ and $A^2\Pi$ potential curves obtained from far-wing intensity measurements of the resonance line of Na broadened by He (Havey et al., 1982) and using the quasi-static approximation to analyze the data. The PP results are in excellent agreement with experiment, while the well depths predicted by the SCF-HF calculations of Krauss et al. (1971) and the MP

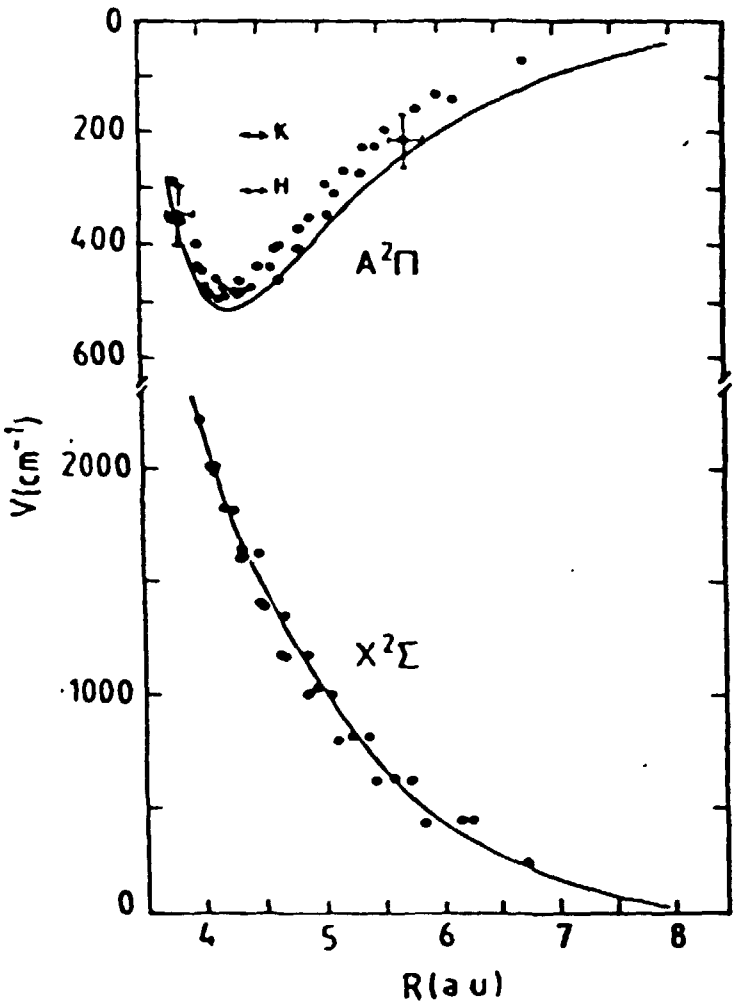

Fig. 2 - $X^2\Sigma^+$ and $A^2\Pi$ potentials of NaHe. Full line : present PP calculations. Full circles : experimental data of Havey et al. (1982). The arrows in the figure indicate minimum of $A^2\Pi$ potential well obtained by HF-SCF (Krauss et al., 1971) and MP (Hanssen et al., 1979) calculations.

calculations of Hanssen et al. (1979) are too small by about a factor of two. The PP results confirmed also the far-red wing intensity measurements of York et al. (1975) which were questioned by the MP calculations. Results for LiHe and KHe indicate the same tendency for the SCF-HF calculations or the MP calculations (using the same e-He model potential as that for NaHe) to underestimate the $A^2\Pi$ well depth (see Table I). In the case of CsHe, the PP calculations improve considerably previous l-independent pseudo-potential (liPP) calculations for both the adiabatic potential

Table I - Position Re(a.u.) and depth De (cm^{-1}) of the $A^2\Pi$ potential wells of LiHe, NaHe and KHe.

Alkali atom	Li		Na		K	
	Re	De	Re	De	Re	De
Method						
SCF-HF[a]	3.5	500	4.53	210		
MP[b]			4.58	299	5.30	190
PP[c]	3.44	1025	4.35	511	5.30	245
Experiment[d]	3.45(.08)	8.50(100)	4.4(.2)	480(50)		

a Krauss et al. (1971).
b NaHe, Hanssen et al. (1979) ; KHe, Masnou-Seeuws (1982).
c J. Pascale (1983).
d LiHe, Balling et al. (1982) ; NaHe, Havey et al. (1982).

energies and the dipole moments. This is seen Figs. 3 and 4 where the PP results are compared with previous liPP calculations and the experimental data of Ferray et al. (1980) derived from absorption measurements in the bands associated with the $^2\Sigma^+$ (6S)-$^2\Sigma^+$ (5D) and $^2\Sigma^+$ (6S)-$^2\Sigma^+$ (5D) transitions. Recently, semiclassical calculations have been performed for these bands (Visticot et al., 1985) using the PP results and the unified Franck-Condon model of Szudy and Baylis (1975). A good overall agreement between experiment and theory was obtained except in the spectral region corresponding to the avoided crossing between the $^2\Sigma^+$ (5D) and $^2\Sigma^+$ (7S) potential curves (see Fig. 3). In this region, the potential curves have to be improved, and the non-adiabatic coupling between the $^2\Sigma^+$ (5D) and $^2\Sigma^+$ (7S) molecular states has to be considered to bring experiment and theory into closer agreement. This has been shown recently by using a Landau-Zener approximation (O'Callaghan et al., 1985).

Recent PM calculations by Mason and Peach (1985) for LiHe and NaHe confirm the good agreement between experimental data and the PP calculations ;

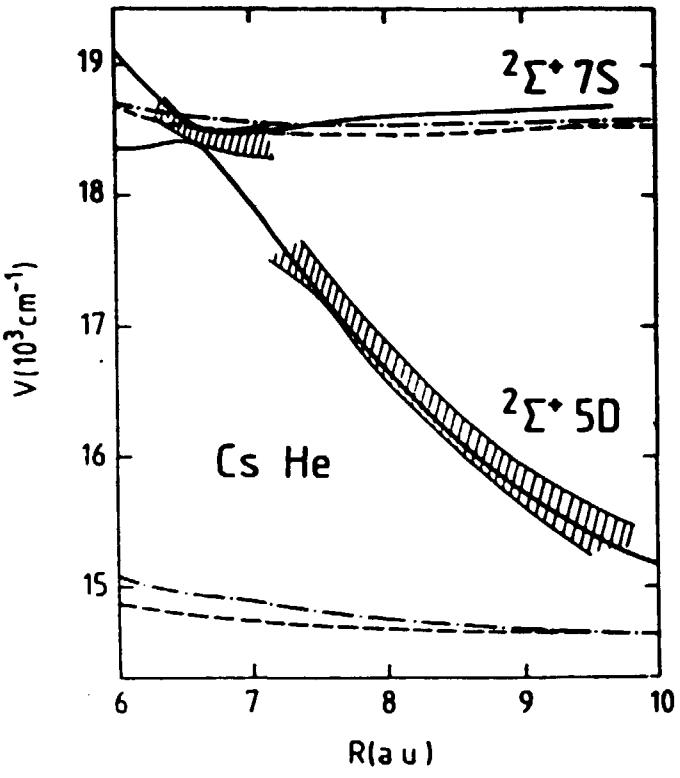

Fig. 3 - Adiabatic potential curves for the $^2\Sigma^+$ (5D) and $^2\Sigma^+$ (7S) states of CsHe. Full line : present PP calculations, dash-dotted line : liPP calculations (Pascale and Vandeplanque, 1974) ; dashed line : liPP calculations (Czuchaj and Sienkiewicz, 1979). Hatching : experimental data (Ferray et al., 1980).

their results for NaNe confirm also the good agreement of the MP calculations of Masnou-Seeuws et al. (1978) with the experimental data of Ahmad-Bitar et al. (1977). This illustrates the difficulty, in the treatment of M-atom-rare gas systems by both the PP and MP methods, of defining correctly the e^--rare gas effective interaction. Additional difficulties arise for the M-atom-heavier rare gas systems, due mainly to an inadequate knowledge of the core core interaction (for a discussion of this problem, see Pascale, 1985) and also because the calculation are more sensitive to the cut-off functions introduced in the expression of the cross-term. Therefore, more work is needed for these systems (in particular, it should be interesting also to evaluate the importance of using a PP approach rather than an liPP approach for the heavier rare gases).

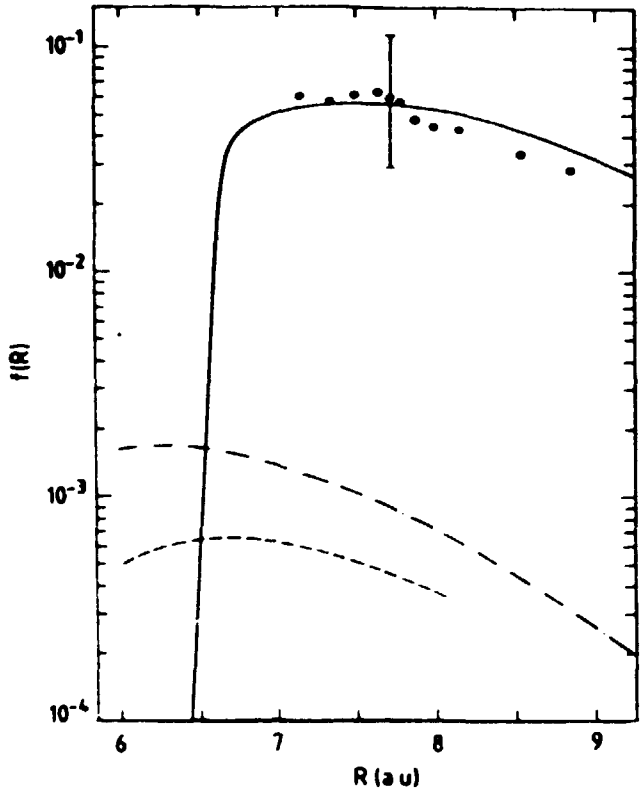

Fig. 4 - Dipole-induced oscillator strength versus R for the $^2\Sigma^+$ (6S)-$^2\Sigma^+$ (5D) transition in CsHe. Full curve : PP calculations (Pascale, 1983) ; dashed-dotted line : liPP calculations (Pascale, 1977) : dashed line : liPP calculations (Czuchaj, 1979). The dots are the experimental data (Ferray et al., 1980).

Treatment of one-electron systems by PP or MP approaches are tending to become standard techniques, in particular for systems such as M-ion-M-atom, alkali-earth ion-rare gas systems, and quite accurate adiabatic energies can be obtained. Treatment of systems as Cd-rare gases or Tl-rare gases is more difficult, but has been considered recently using a liPP approach (Czuchaj and Sienkiewicz, 1984 and 1985). Extensions of the PP and MP methods to systems with two or more valence electrons is relatively straightforward, but the treatment of the valence-electron correlations requires additional effort. Moreover, for systems with more than one electron, the PP approach should be preferred to the MP approach, as discussed above. Studies on M-atom-M-atom and alkali earth-rare gas systems are

presently in progress in several laboratories. Finally, treatment of polyatomic systems by PP or MP approaches is certainly possible, but calculations are more difficult than for diatomic systems because of the many-center integrals to evaluate. In the following section, we present the first detailed calculations on M-atom-H_2 systems using a PP approach, in which H_2 has been treated as a one-center system and anisotropic terms have been defined to account for the molecular structure of H_2 (Rossi and Pascale, 1985).

B.2 - M-atom-H_2 systems. In the PP approach of these systems, a one-electron two-center model has been considered (see Fig. 5) in which the valence

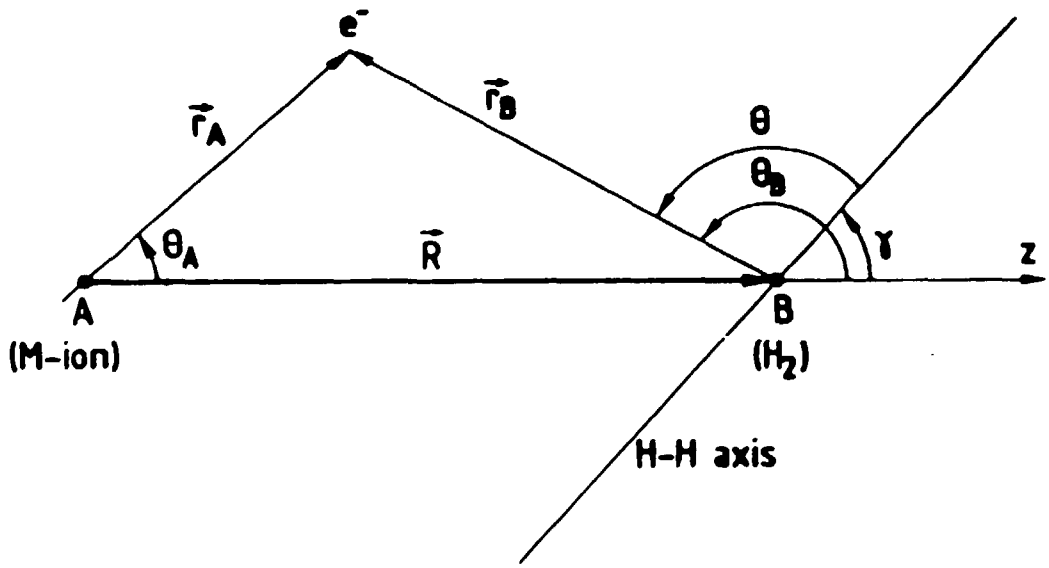

Fig. 5 - The one-electron two-center model describing the M-atom-H_2 system.

electron e^- and the M-ion (core A) interact with an anisotropic core B representing H_2. The molecule H_2 is assumed to be in its ground state $X^1\Sigma_g^+$ (v=0) and therefore the distance between the two protons of H_2 is assumed to correspond to the equilibrium distance r_e = 1.4 a.u.. The angle γ specifies the orientation of the H-H axis with respect to the core-core AB axis taken as quantization axis. The problem is now to determine the

electronic energies $E_{el}(R,\gamma)$ by solving the one-electron Schrödinger equation,

$$H_{el}\,\psi_{el} = E_{el}(R,\gamma)\,\psi_{el}\ , \tag{24}$$

for any given distance R and angle γ. Then, the adiabatic potential energies $E(R,\gamma)$ are obtained by adding to $E_{el}(R,\gamma)$ the core-core interaction $V_{AB}(R,\gamma)$. As for the M-He system, the one-electron Hamiltonian is defined as

$$H_{el} = -\frac{1}{2}\nabla^2_{\vec{r}_X} + V_A + V_B + V_{CT}\,(\vec{r}_X,\vec{R},\gamma) \tag{25}$$

where again the cross term V_{CT} has to be included to have the correct behavior of $E(R,\gamma)$ at large R-values.

B.2.a - The interactions. V_A is the operator previously defined for the M-He system (see Section B.1.a). The operator V_B describing the e^--H_2 interaction was considered, as above, as the the sum of a long-range part V_B^{LR} (which is well-known asymptotically) and of a short-range part V_B^{SR}. $V_B{}^{LR}$ was limited to terms in R^{-4}, corresponding to anisotropic terms in $P_2(\cos\theta)$:

$$V_B^{LR} = -\frac{1}{2}\frac{\alpha^{(o)}_{d_B}}{(r_B^2 + d_B^2)^2} - \left(\frac{1}{2}\frac{\alpha^{(2)}_{d_B}\, r_B^2}{(r_B^2 + d_B^2)^2} + \frac{Q\, r_B^3}{(r_B^2 + d_B^2)^3}\right) P_2(\cos\theta) \tag{26}$$

where $\alpha^{(o)}_{d_B} = 5.18$ a.u. and $\alpha^{(2)}_{d_B} = 1.2$ a.u. (Kolos and Wolniewicz, 1967) are the isotropic and anisotropic static dipole polarizabilities, respectively, and $Q = 0.49$ a.u. (Karl and Poll, 1967) the quadrupole moment of H_2 in its ground state $X\,{}^1\Sigma_g^+$ (v=o). d_B is a cut-off radius fixed to a value of 1.6 a.u. (Hara, 1967). As for the e^--He interaction, the role of V_B^{SR} is mainly to simulate the Pauli principle. Therefore, the isotropic pseudopotential previously defined for the e^--He interaction was generalized by introducing an angular dependence in θ, which has been limited to terms in $P_2(\cos\theta)$ to be consistent with V_B^{LR}, and

$$V_B^{SR} = \sum_{l=0}^{\infty} V_{Bl}^{(o)}(r_B)\mathcal{P}_l^B + \sum_{l=0}^{\infty} V_{Bl}^{(2)}(r_B)\frac{1}{2}\{P_2\cos\theta), \mathcal{P}_l^B\}\ . \qquad (27)$$

The anticommutator { } ensures the Hermiticity of H_{el}, and $V_{Bl}^{(o),(2)}(r_B)$ are Gaussian-type radial operators (see, Eq. (16)). The coefficients determining V_B^{SR} were adjusted to reproduce the experimental data of Linder and Schmidt (1971) concerning the differential elastic scattering of e^- with H_2 in its ground state $X^1\Sigma_g^+$ (v=o), as well as the theoretical value 1.27 a.u. determined by Chang (1981) for the scattering length. As seen in Fig. 6, the limitation of the l-dependence of the pseudopotential to l = 0,1, as for the e^--He interaction, was sufficient to obtain good agreement with scattering experimental data.

The cross-term V_{CT} which results from the polarization of H_2 by both the point charges e^- and the M-ion is well-known asymptotically (see, for example, Buckingham, 1967), and it is taken as :

$$V_{CT}(\vec{r}_A,\vec{R},\gamma) = -\left[\frac{\alpha_{d_B}^{(o)}\cos\theta_B}{(R^2+d_B^2)(r_B^2+d_B^2)} + \frac{\alpha_{d_B}^{(2)} r_B R(3\cos\theta\cos\gamma - \cos\theta_B)}{2(R^2+d_B^2)^{3/2}(r_B^2+d_B^2)^{3/2}}\right] f_c\left(\frac{R}{r_A}\right) \qquad (28)$$

where cut-off functions have been introduced consistently with the definition of V_B^{LR} above and that of $V_{AB}(R,\gamma)$ below ; the same additional cut-off function $f(\frac{R}{r_A})$ previously defined for the M-He systems was also used.

Finally, in order to calculate the adiabatic potential energies $E(R,\gamma)$, the core-core interaction $V_{AB}(R,\gamma)$ has to be determined. An approach similar to that used for calculating the M-ion-He interaction (based on the knowledge of the interaction asymptotically and its determination at short R-values from high-energy elastic scattering experiments) is not possible for the M-ion-H_2 systems since the scattering data are averaged over the angle γ. In order to estimate $V_{AB}(R,\gamma)$, a method has been proposed (Rossi

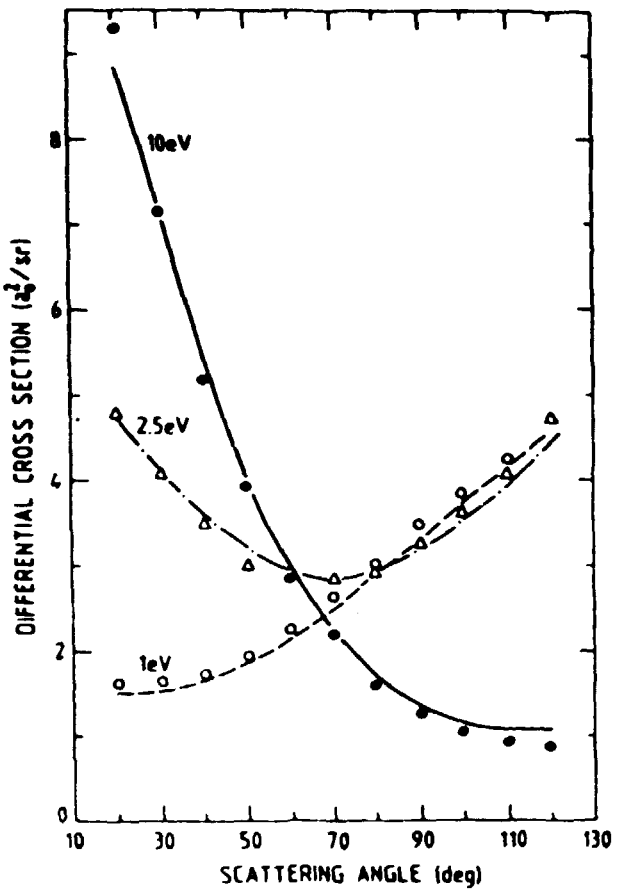

Fig. 6 - Calculated differential cross sections versus scattering angle for the elastic scattering of e^- by H_2 in its ground state $X^1\Sigma_g^+$ (v=o), for three energies as indicated in the figure. The symbols are the experimental points of Linder and Schmidt (1971).

and Pascale, 1985). It consists of writting $V_{AB}(R,\gamma)$ as,

$$V_{AB}(R,\gamma) = V_{static}(R,\gamma) + V_{induction}(R,\gamma) + V_{dispersion}(R,\gamma) \ . \qquad (29)$$

The last two terms of expression (29) can be easily obtained (see, for example, Buckingham, 1967) :

$$V_{induction}(R,\gamma) = - \frac{\alpha_{d_B}^{(o)}}{2\,(R^2 + d_B^2)^2} - \frac{\alpha_{d_B}^{(2)}\ R^2}{2\,(R^2 + d_B^2)^3}\ P_2\,(\cos\gamma) \ , \qquad (30)$$

and

$$V_{dispersion}(R,\gamma) = -\frac{3}{2} F \left[\frac{\alpha_{d_A} \alpha^{(o)}_{d_B}}{(R^2 + d_A^2)^{3/2} (R^2 + d_B^2)^{3/2}} + \frac{1}{2} \frac{\alpha_{d_A} \alpha^{(2)}_{d_B} R^2 P_2 (\cos \gamma)}{(R^2 + d_A^2)^2 (R^2 + d_B^2)^2} \right], \quad (31)$$

where the factor F in Eq. (31) is determined by the Slater-Kirkwood formula (1931). An estimation of $V_{static}(R,\gamma)$ can be obtained by considering the first-order term of a stationary perturbative method. It consists of taking the average value, with respect to an approximate wave function describing H_2 in its ground-state $X^1\Sigma_g^+$ (v=o) (Hara, 1967), of the sum of the interactions between the M-ion and each of the particles constituting H_2. The interaction between an electron and the M-ion is taken to be the sum of V_A^{SR} previously defined and of the Coulombic interaction ; the interaction between a proton and the M-ion is taken as the sum of the Coulombic interaction and of minus $V_{A1_{max}}^{SR}$, where 1_{max} has been defined above (see Chapter 2.A.3). It was found that this approach leads to an underestimation of the quadrupole moment for H_2. Then, to remedy this problem, $V_{static}(R,\gamma)$ was taken as

$$V_{static}(R,\gamma) = V'_{static}(R,\gamma) + \frac{Q R^3}{(R^2 + d_B^2)^3} P_2 (\cos \gamma) \quad (32)$$

where V'_{static} is calculated as above, but where the Coulombic part of the interaction is replaced by the first order term of its expansion in terms of Legendre polynomials $P_1 (\cos \gamma)$. A good overall agreement with previous *ab initio* calculations was then found for Li^+H_2 and Na^+H_2 for the two symmetries $C_{\infty v}$ and C_{2v} which were considered (Rossi and Pascale, 1985).

B.2.b - Molecular-structure calculations. The large basis set of STO's centered on the M-ion previously defined for the treatment of the M-atom-He systems was also used for the M-atom-H_2 systems. The calculations were

performed for the $C_{\infty v}$ and C_{2v} symmetries. In the $C_{\infty v}$ symmetry (γ=0), the classification of the molecular states is identical to that for the M-atom-He systems, and the $^2\Sigma$, $^2\Pi$, $^2\Delta$, etc..., result from diagonalization of the electronic Hamiltonian H_{el} for each class of states. In the C_{2v} symmetry ($\gamma = \frac{\pi}{2}$), the molecular states of the M-atom-H_2 system separate in classes $^2A_1$, $^2B_1$, $^2B_2$ and $^2A_2$, and their adiabatic energies are similarly obtained from diagonalization of H_{el} for each class of states.

B.2.c - Results and discussion. No experimental data are presently available for the M-H_2 systems for testing the validity of the PP calculations. Therefore, comparisons with accurate *ab initio* results, when available, are quite valuable. The *ab initio* calculations of Botschwina et al. (1981) for the first lowest states of NaH_2, for R_{H-H} = 1.4 a.u. corresponding to the condition of the PP calculations, are very instructive. These authors have used the restricted-Hartree-Fock (RHF)-SCF method as a first step. Then, calculations were repeated for the X^2A_1 and A^2B_2 potential curves using the paired-natural-orbitals-coupled-electron-pair-approximation (PNO-CEPA) method, which takes into account most of the electronic correlations. The *ab initio* results are shown in Figs. 7 and 8 for the C_{2v} and $C_{\infty v}$ symmetries, respectively, along with the PP results. While the X^2A_1 potential curve is little changed from the RHF-SCF results, the A^2B_2 potential curve is found more attractive when calculated using the PNO-CEPA method. Therefore, the good agreement which is observed between the PNO-CEPA and PP results (see Fig. 7), in particular for the A^2B_2 potential curve, is quite significative since the PP approach takes implicitely into account correlation effects through the use of experimental core polarizabilities. As expected, the PP adiabatic potential energies are generally lower than the energies obtained by the RHF-SCF method. For the B^2A_1 and $B^2\Sigma^+$ potential curves, however, where repulsive effects are predominant and the correlation effects less important, a good agreement is observed between PP and RHF-SCF results. This tendency of the PP approach to find (in agreement with more sophisticated calculations) adiabatic energies which are generally lower than those obtained from RHF-SCF calculations was already observed for the M-atom-He systems (see, Sec. B.1.c). The comparisons of the PP results with the HF-SCF calculations of Krauss (1968) for the LiH_2

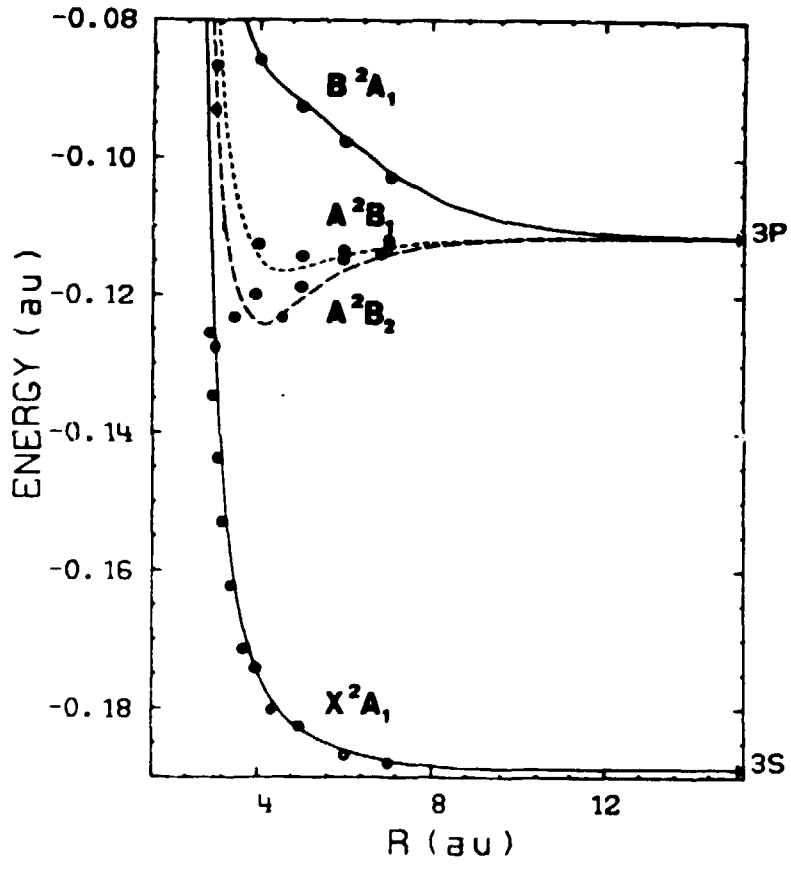

Fig. 7 - Adiabatic potential energies for the lowest states of NaH_2 in C_{2v} symmetry. PP results are compared with RHF-SCF (open circles) and PNO-CEPA (full circles) calculations of Botschwina et al. (1981).

system are consistent with these observations (see, Figs. 9 and 10), considering the *ab initio* calculations were performed for a distance R_{H-H} = 1.5 a.u. corresponding to an absolute minimum in the A^2B_2 potential curve (similar calculations for R_{H-H} = 1.4 a.u. should increase the energy values). The results of Wagner et al. (1978) for the X^2A_1 and $X^2\Sigma^+$ potential curves, obtained from multiconfiguration-self-consistent-field-optimized-valence-configurations (MCSCF-OVC) calculations, are also shown in Figs. 9 and 10. These calculations illustrate again the difficulty for *ab initio* calculations to take correlation effects correctly into account. Comparisons with the PP results show a good agreement for the X^2A_1 potential curve, while the PP $X^2\Sigma^+$ potential curve is found less repulsive.

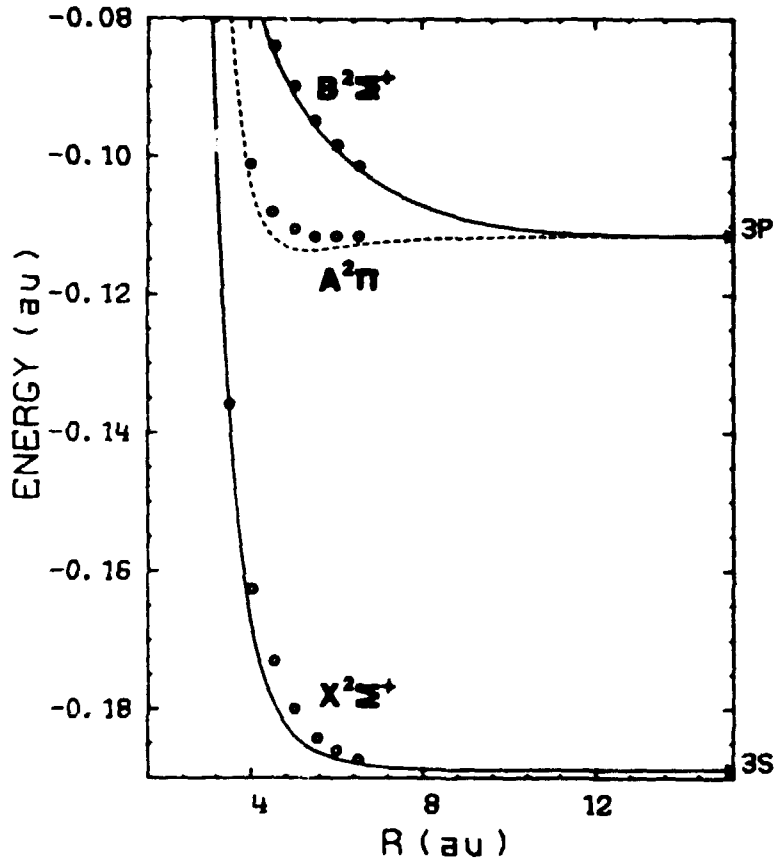

Fig. 8 - Adiabatic potential energies for the lowest states of NaH_2 in $C_{\infty v}$ symmetry. As in Fig. 7.

This good overall agreement between the PP results and available *ab initio* results (in general, considering the most sophisticated of them) allows us to have some confidence in the validity of the PP predictions for the M-atom-H_2 systems. Note that for CsH_2, preliminary calculations of Gadea et al. (1983) using an *ab initio* pseudopotential method are only in qualitative agreement with present PP calculations, the adiabatic energies obtained by this method being much lower than those obtained by the PP approach.

In view of the rather encouraging results obtained for the M-atom-H_2 systems by using the PP two-center approach, treatment of other systems (M-atom-N_2 systems, for example) by the same approach could be envisaged. However, in order to study reactive collisional problems, the present

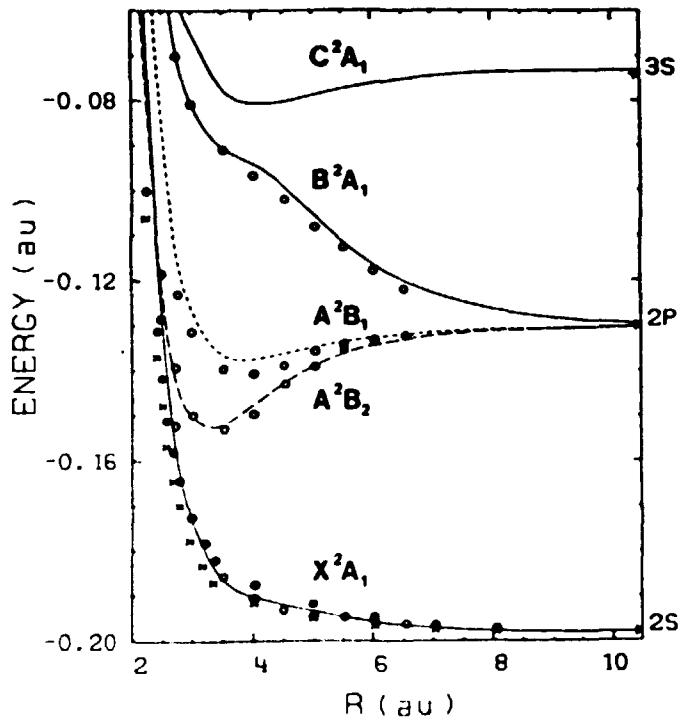

Fig. 9 - Adiabatic potential energies of the lowest states of LiH_2 in C_{2v} symmetry. The PP results are compared with HF-SCF calculations of Krauss (1968), open circles ; and with MCSCF-OVC calculations of Wagner et al. (1978) for two levels of approximation (15 OVC, crosses ; 28 OVC, full circles).

approach should be extended to a three-center model in which the interaction between a valence electron and each center is described by an l-dependent pseudopotential.

3. Applications of the PP approach to the study of atom-atom collisions

In the following, we show that the use of the PP approach in molecular-structure calculations of the M-atom-He systems allows us a systematic study (from Li to Cs) of some collisional processes involving the M-atom. First, the PP molecular-structure calculations have been applied to extensive cross-section calculations concerning intra-n^2P transitions induced in thermal or suprathermal collisions of the M-atoms with He in its ground-

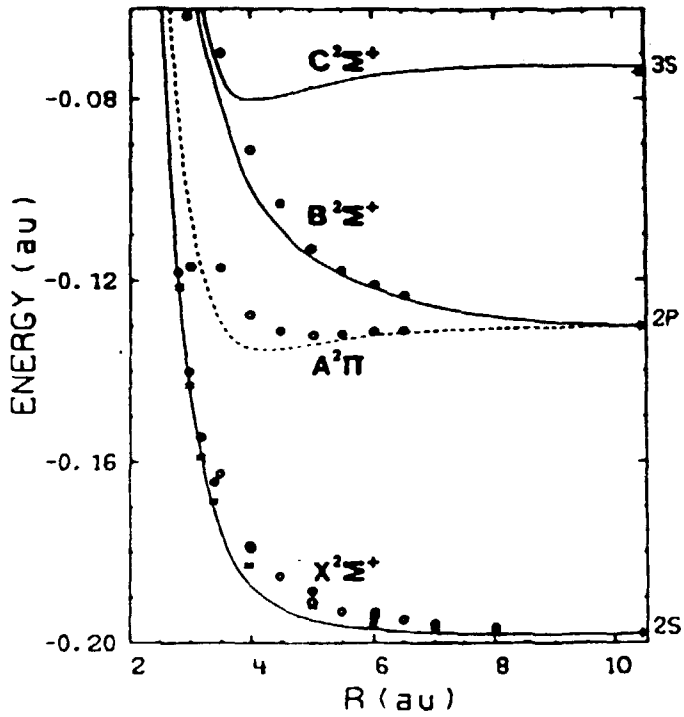

Fig. 10 - Adiabatic potential energies of the lowest states of LiH_2 in $C_{\infty v}$ symmetry, as in Fig. 9.

state. Second, extensive calculations concerning the transition from the ground-state to the first n^2P level of the M-atoms, in the keV energy range, have been performed allowing us to complete the test of the PP molecular-structure calculations against experimental scattering data.

A - *Intra-n^2P transitions in the M-atom, in thermal or suprathermal collisions with He*

Quantum-mechanical calculations of cross-sections for $n^2P_{1/2} \rightleftarrows n^2P_{3/2}$ transitions in M-atom collisions with He in its ground state have been performed in the energy range from threshold of the fine-structure transition up to 0.5 eV. More generally, the cross-sections for the $n^2P_{jm} \rightleftarrows n^2P_{j'm'}$, Zeeman transitions have been calculated, which allows us to determine any observable. The first n^2P level of all M-atoms, and the second and third n^2P levels of Rb and Cs have been investigated (Pascale,

1983c). The calculated total cross sections are compared with various experimental data : cell-type experimental data, requiring the average of the calculated cross sections over the Maxwell-Boltzman distribution of velocities ; crossed-beam experimental data, sometimes with the evaluation of polarization effects.

A.1 - Theory. In the quantum-mechanical formulation of the scattering problem, one has to solve the Schrödinger equation,

$$H\psi = E\psi \tag{33}$$

where E is the total energy of the system and :

$$H = -\frac{1}{2\mu}\nabla^2_{\vec{R}} + H_A + V(\vec{r},\vec{R}) \ , \tag{34}$$

and to consider the asymptotic behavior of the wave function Ψ which determines the T-matrix, allowing us to calculate the cross-sections of the intra-n^2P transitions. In Eq. (34), H_A is the one-electron Hamiltonian for the M-atom, including the spin-orbit interaction ; $V(\vec{r},\vec{R})$ is the M-atom-rare gas interaction (equal to $V_B + V_{AB} + V_{CT}$ defined above) ; and μ is the reduced mass of the system.

For intra-n^2P transitions induced in M-atom collisions with a rare gas, the quantum-mechanical formulation (see Reid, 1973) follows the theory of Arthurs and Dalgarno (1960) for the collisional excitation of a rigid-rotator, where the rigid-rotator wave function is replaced by the valence electron wave function. It takes advantage of the fact that $V(\vec{r},\vec{R})$ can be expanded in Legendre polynomials,

$$V(\vec{r},\vec{R}) = \sum_{\lambda=0}^{\infty} v_\lambda (r,R)\ P_\lambda (\hat{r}.\hat{R}) \tag{35}$$

Then, assuming the n^2P level is well isolated in the energy diagram of the M-atom, so that its wave function is little perturbed during the collision, only the $\lambda = 0, 2$ terms are involved in the calculations. This assumption is well justified for the first n^2P level, and numerous calculations have been performed in that case. Recently (Pascale, 1983c) the

theory has been applied to the second and third n^2P levels of Rb and Cs in collisions with He because their wave functions were found also little perturbed in the region $R > 8$ a.u. which mainly contributes to the intra-n^2P transitions.

The scattering problem is formulated in a space-fixed axis system, and the scattering wave function ψ is taken to be an eigenfunction of J^2 and J_z since H commutes with the total angular momentum of the system,

$$\vec{J} = \vec{j} + \vec{l} \tag{36}$$

where $\vec{j}$ is the total angular momentum of the M-atom and $\vec{l}$ is the angular momentum for the relative motion of the system. Next, by expanding ψ in terms of eigenfunctions ϕ^{JM}_{jl} of J^2, J_z, j^2 and l^2,

$$\psi^{JM}_{j_1 l_1}(\vec{r}, \sigma, \vec{R}\,; E) = \sum_{jl} \frac{1}{R} F^{JE}_{jl\, j_1 l_1}(R)\, \phi^{JM}_{jl}(\vec{r}, \sigma, \hat{R}) \tag{37}$$

two sets of, at most, three coupled equations result :

$$\left[\frac{d^2}{dR^2} + k_2^2 - \frac{l_2(l_2+1)}{R^2}\right] F^{JE}_{j_2 l_2\, j_1 l_1} = \frac{2\mu}{\hbar^2} \sum_{jl} V^{J}_{j_2 l_2\, jl}\, F^{JE}_{j_2 l_2\, j_1 l_1} \tag{38}$$

where k_2 is the wavenumber of the relative motion in the j_2-channel. In Eq. (37), σ is a spin variable, and j_1, l_1 specifv the initial conditions. The matrix elements $V^{J}_{j_1 l_1 jl}$ are non-zero for $|l-l_1|$ even, and can be explitily written in terms of 3-j and 6-j coefficients, and in terms of $\hat{v}_{\lambda=0,2}(R)$ (the expectation value of $v_{\lambda=0,2}(r,R)$ over the radial wave function of the n^2P level. The terms $\hat{v}_{\lambda=0,2}(R)$ may be evaluated from the $^2\Sigma$ and $^2\Pi$ PP adiabatic potential energies relative to the n^2P level :

$$\hat{v}_0(R) = \frac{1}{3}\left(E_\Sigma(R) + 2\,E_\Pi(R)\right) \tag{39}$$

and

$$\hat{v}_2(R) = \frac{5}{3}\left(E_\Sigma(R) - E_\Pi(R)\right) \tag{40}$$

For a given value of E (relative to the $n^2P_{1/2}$ level), the two coupled-equation sets (Eq. (38)) are solved under standard boundary conditions and the $T^J(j_2l_2 ; j_1l_1)$ matrix and then the total cross section for the $j_1m_1 \rightarrow j_2m_2$ transition are obtained :

$$\sigma_{j_1m_1\rightarrow j_2m_2}(E;\hat{k}_1) = \frac{4\pi^2}{k_1^2} \sum_{l_1l_2lM} (i)^{l_1-l} Y^*_{l_1,M-m_1}(\hat{k}_1)\, Y_{l,M-m_1}(\hat{k}_1) G_{l_1l_2M} G^*_{ll_2M} \tag{41}$$

where G is defined as (Mies, 1973)

$$G_{l_1l_2M} = \sum_J \langle j_1l_1M-m_1 \,|JM\rangle\, T^J(j_1l_2;j_1l_1)\, \langle j_2l_2m_2M-m_2|JM\rangle \tag{42}$$

Two types of cross-sections are then defined for purpose of comparisons with experimental data.

For cell-type experiments, one has to average over all orientations of $\hat{k}_1$ with respect to the space-fixed z-axis, and one defines the cross-section $\bar{\sigma}$,

$$\bar{\sigma}(j_1m_1 \rightarrow j_2m_2) = \frac{\pi}{k_1^2} \sum_{l_1l_2M} G_{l_1l_2M}\, G^*_{l_1l_2M} \tag{43}$$

which obeys both detailed balance and the relation $\bar{\sigma}(j_1m_1 \rightarrow j_2m_2) = \bar{\sigma}(j_1-m_1 \rightarrow j_2-m_2)$ in absence of a magnetic field. However, the observables which are more usually measured in cell-type experiments are the multipole relaxation cross sections $\sigma_j^{(x)}$ which are derived from the general matrix theory of collisional relaxation (see, for example, Baylis, 1979)

$$\sigma_j^{(x)} = \Lambda_j^{(x)} + \sigma(j \rightarrow j' \neq j) \tag{44}$$

where $\Lambda_j^{(o)} = 0$ and the $\Lambda_j^{(x\neq o)}$ are related to the Zeeman cross sections $\bar{\sigma}(j_1m_1 \rightarrow j_2m_2)$. The second term in Eq. (44) is the fine-structure transition cross-section. For purpose of comparison with experiment, all these cross-sections have to be thermally averaged.

For crossed-beam type experiments, the orientation of $\hat{k}_1$ with respect to

the z-axis has to be specified ; usually, one takes $\hat{k}_1$ along the z-axis and one defines the cross-section σ_o,

$$\sigma_o (j_1 m_1 \to j_2 m_2) = \frac{\sigma}{k_1^2} \sum_{l_1 l_2 l} i^{l_1 - l} (2l_1+1)^{1/2} (2l+1)^{1/2} G_{l_1 l_2 m_1} G^*_{l l_2 m_1} \tag{45}$$

This cross section does not generally obey detailed balance but one has always the relation $\sigma_o(j_1 m_1 \to j_2 m_2) = \sigma_o (j_1 - m_1 \to j_2 - m_2)$ in absence of a magnetic field. Finally, from Eq. (43) or Eq. (45) the conventional fine-structure transition cross-section may be defined :

$$\sigma (j_1 \to j_2) = \frac{1}{2j_1+1} \sum_{m_1, m_2} \sigma_o (j_1 m_1 \to j_2 m_2) \tag{46a}$$

$$= \frac{1}{2j_1+1} \sum_{m_1, m_2} \bar{\sigma} (j_1 m_1 \to j_2 m_2) \tag{47a}$$

However, in a crossed-beam experiment, polarization effects may be important (see, Pascale and Perrin, 1980 ; Pascale et al., 1984) and they have to be considered for comparison with experimental data. Thus, for the crossed-beam experiment of Mestdagh et al. (1982) concerning the $K(4^2P)$ + He collision, and where the K-beam is excited from the $4^2S_{1/2}$, F = 2 level to the $4^2P_{3/2}$, F = 3 level, the measured apparent fine-structure transition cross-section $\sigma^{(a)}(\frac{3}{2} \to \frac{1}{2})$ was found (for the particular geometry of this experiment) to be :

$$\sigma^{(a)}(\tfrac{3}{2} \to \tfrac{1}{2}) = \frac{1}{4} \sum_{m_2} \left[\sigma_o(\tfrac{3}{2}\,\tfrac{3}{2} \to \tfrac{1}{2}\, m_2) + 3\, \sigma_o(\tfrac{3}{2}\,\tfrac{1}{2} \to \tfrac{1}{2}\, m_2)\right] \tag{48}$$

in place of the conventional cross-section $\sigma^{(c)}(\frac{3}{2} \to \frac{1}{2})$,

$$\sigma^{(c)}(\tfrac{3}{2} \to \tfrac{1}{2}) = \frac{1}{2} \sum_{m_2} \left[\sigma_o(\tfrac{3}{2}\,\tfrac{3}{2} \to \tfrac{1}{2}\, m_2) + \sigma_o(\tfrac{3}{2}\,\tfrac{1}{2} \to \tfrac{1}{2}\, m_2)\right] \tag{49}$$

In the following, some results that we judge particularly illustrative of these quantum mechanical calculations are reported.

A.2 - First n^2P levels. Calculations have been carried out for the first n^2P level of all the M-atom, for which the spin-orbit energy splitting $\Delta\varepsilon$ ranges from 0.34 cm^{-1} for $Li(2^2P)$ to 554 cm^{-1} for $Cs(6^2P)$.

Figure 11 shows the $\hat{v}_2(R)$ terms for all the M-atom-He systems calculated from the above reported PP calculations. These terms are essential for determining the intra-n^2P transitions. Indeed, in a semiclassical approach

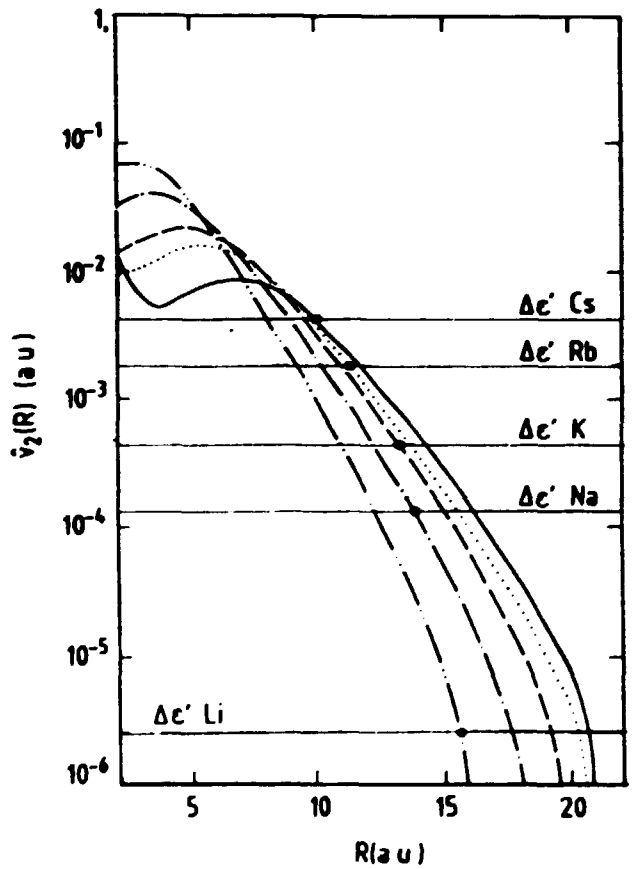

Fig. 11 - $\hat{v}_2(R)$ for all M-atom-He systems (see text). Full curve : Cs, dotted curve : Rb ; dashed curve : K ; dot-long-dashed curve : Na ; double dot-long-dashed curve : Li. The full circles indicate the position of maxima in radial coupling predicted by Eq. (50) and $\Delta\varepsilon' = 5/3\ \Delta\varepsilon$.

of the problem (see, Nikitin, 1975 and references therein), it is shown that fine-structure transitions are mainly induced in the region of a non-adiabatic coupling (radial coupling) between the two $\Omega = 1/2$ molecular

states (where Ω denotes the absolute value of the projection of the total angular momentum $\vec{j}$ of the M-atom along the internuclear axis) associated with the $n^2P_{1/2}$ and $3/2$ levels, and determined by the condition

$$| \hat{v}_{2}(R_1) | = \frac{5}{3} \Delta\varepsilon \qquad (50)$$

This non-adiabatic coupling results from the breakdown of the spin-orbit interaction. This is clearly seen in Fig. 12, for the LiHe system as an

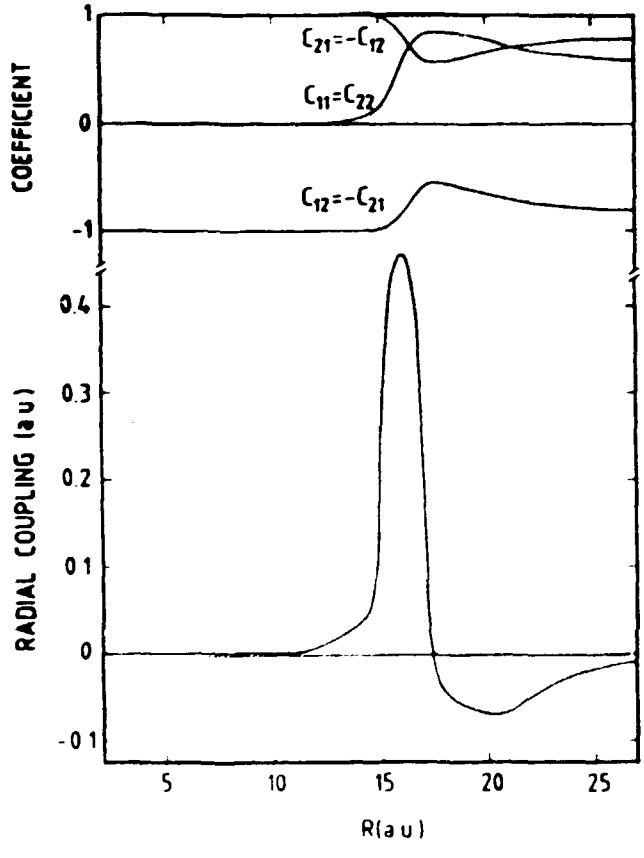

Fig. 12 - Radial coupling between the Ω = 1/2 adiabatic molecular states associated to the 2^2P_j levels, for the Li-He system, and coefficients $C_{ij}(R)$ of the expansion of the Ω = 1/2 molecular wave functions $\psi_i^{1/2}$ in terms of the wave functions for the $B^2\Sigma^+$ and $A^2\Pi$ molecular states (see text).

example, where the radial coupling is seen to have a large maximum in the region R_1 predicted by Eq. (50). Fig. 12 shows also the coefficients of the expansion of the two $\Omega = 1/2$-molecular wave functions $\psi_i^{1/2}$ in terms of appropriate tensorial products of spin functions α or β and the molecular wave function ψ^1 and ψ^0 corresponding to the $A^2\Pi$ and $B^2\Sigma^+$ molecular states :

$$\psi_i^{1/2}(\vec{r},R) = C_{i1}(R)\ \psi^0(\vec{r},R) \otimes \alpha + C_{i2}(R)\ \psi^1(r,R) \otimes \beta \qquad (51)$$

where $C_{11} = C_{22}$ and $C_{12} = -C_{21}$ ($i = 1$ corresponds to the $^2P_{1/2}$ level, and $i = 2$ to the $^2P_{3/2}$ level). It is clearly seen that for $R < R_1$ one of the two $\Omega = 1/2$ molecular states becomes a pure Π state, while the other one becomes a pure Σ state. Fig. 12 shows also a secondary maximum in the radial coupling, corresponding to the crossing of the $A^2\Pi$ and $B^2\Sigma^+$ poten-

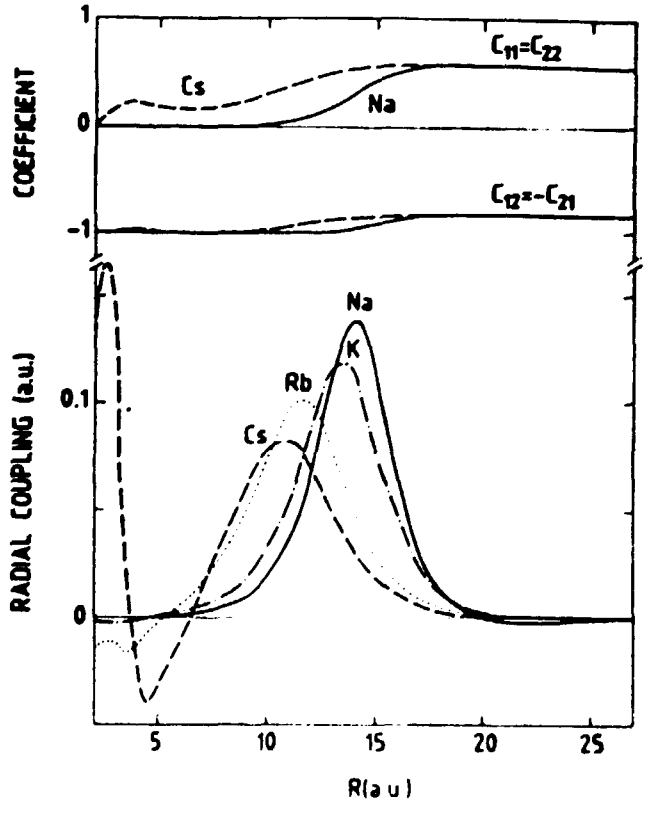

Fig. 13 - Radial coupling and coefficients $C_{ij}(R)$, as in Fig. 12, for the M-atom-He systems as indicated in the figure.

tial curves at large R. When the M-atom changes from Li to Cs, R_1 decreases from about 15.5 a.u. to 10.0 a.u. ; but while the main radial coupling decreases in magnitude, it spreads out more and more around its corresponding position R_1 (because the spin-orbit decoupling takes place more and more slowly as seen in Fig. 13). This explains why the cross sections for the $n^2P_{1/2} \rightarrow n^2P_{3/2}$ transitions reach more and more rapidly a plateau with increasing energy (see Fig. 14) when going from Li to Cs ; and why this

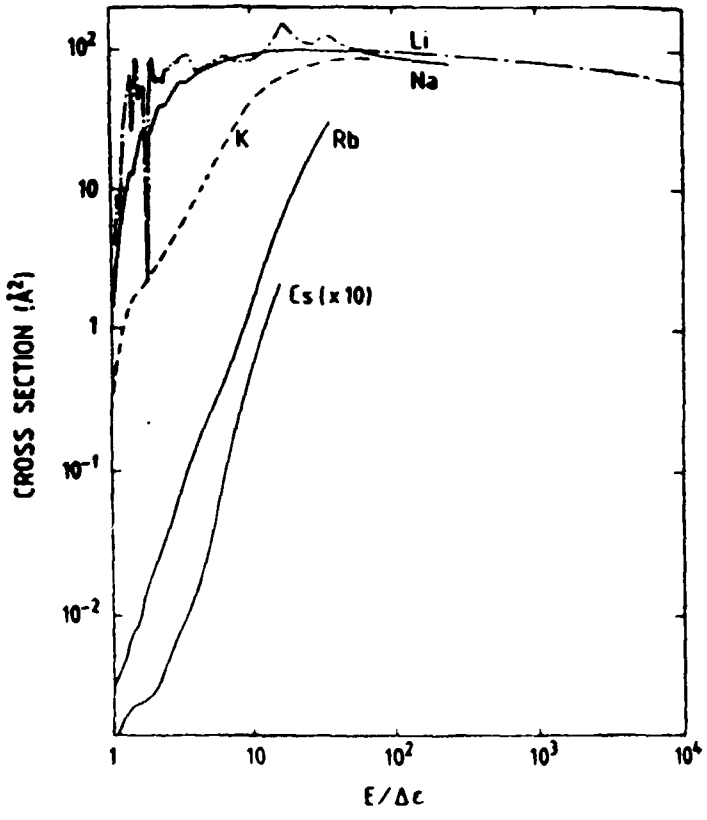

Fig. 14 - Cross sections for the $n^2P_{1/2} \rightarrow n^2P_{3/2}$ transition in the M-atom (as indicated in the figure) in collisions with He versus $E/\Delta\varepsilon$, where E is the collision energy and $\Delta\varepsilon$ the spin-orbit plitting of the n^2P level.

plateau does not change too much in magnitude. A pronounced resonance structure is also observed, at low energies, in the fine-structure cross section for Li ; it is primarily due to orbiting in the $A^2\Pi$ adiabatic potential. Finally, it is worthwhile to mention that, in the case of the

M-atom-He collisions, rotational coupling between the 1/2 and 3/2 molecular states (emerging from the $A^2\Pi$ state when spin-orbit is considered) contributes also to the fine structure transition. This rotational coupling, which generally occurs at small R-values where the potential curves are repulsive (Nikitin, 1975) is found to extend to relatively larger R-values for these systems.

Before comparing some results of the quantum-mechanical calculations with experimental data, let us discuss the relative magnitude of the thermal averaged cross sections for disorientation, namely the 1/2 1/2 → 1/2 -1/2 and 3/2 3/2 → 3/2 -3/2 transitions, when going from Li to Cs (see Fig. 15). The 3/2 3/2 → 3/2 -3/2 cross section increases by about three order in

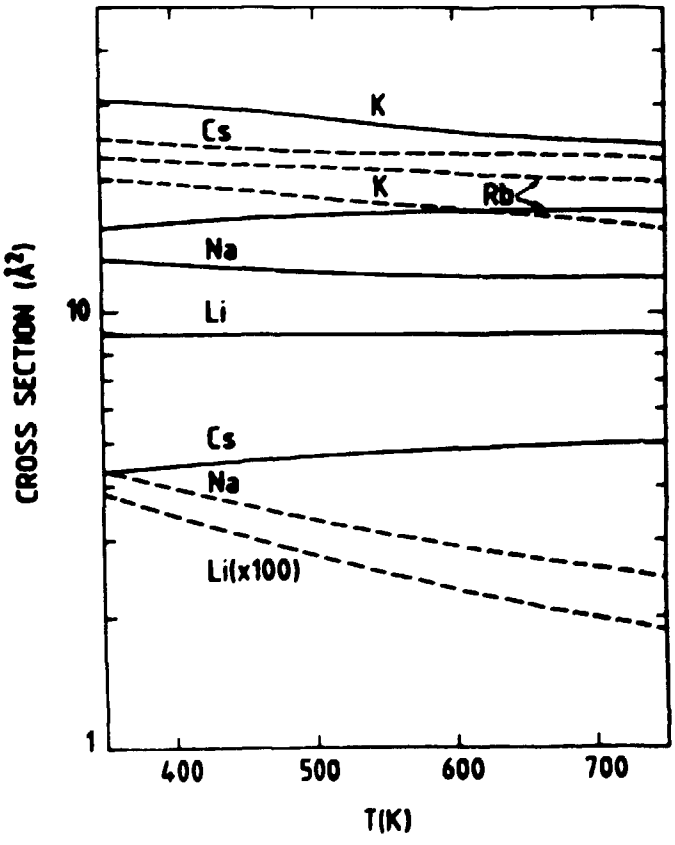

Fig. 15 - Thermal averaged cross sections for 1/2 1/2 → 1/2 -1/2 (full line) and 3/2 3/2 → 3/2 -3/2 (dashed line) transitions in the first n^2P level of the M-atom (as indicated in the figure) in collisions with He, versus temperature.

magnitude from Li to Cs, while the 1/2 1/2 → 1/2 -1/2 cross section goes through a maximum for K and only changes by about one order of magnitude. This can be understood by considering the ratio of the collision time, $\tau_c = \frac{a}{v}$ (where a is the range of the M-atom-He interaction and v the relative velocity of the system), to the spin-orbit coupling time, $\tau_{s.o} = \Delta\varepsilon^{-1}$. This ratio is about 3.10^{-2}, 2, 5, 18 and 39, respectively, for Li, Na, K, Rb and Cs. This means that during the collision with He, the orbital angular momentum $\vec{L}$ and the spin $\vec{S}$ are indeed uncoupled for Li, and strongly coupled for Rb and Cs, while for Na and K the situation is intermediate. So, the disorientation cross section should be the smallest for Li and the largest for Cs. This is indeed observed for the 3/2 3/2 → 3/2 -3/2 transitions. In the case of the 1/2 1/2 → 1/2 -1/2 transitions, which are only allowed through transition to the the $^2P_{3/2}$, the maximum of the cross section for K is explained by the rapid decrease of the fine-structure transition cross section when going from Li to Cs.

Table II - Thermal averaged cross sections in $\mathring{A}^2$ (T = 450 K) for Zeeman transitions in Na (3^2P_{jm}) + He collisions. Comparison of calculated cross sections (Pascale, 1983b) with experimental data of Gay and Schneider (1976).

Transitions	Present results	Experiment
$1/2 \pm 1/2 \rightarrow 1/2 \mp 1/2$	12.55	13.2 ± 1.8
$1/2 \pm 1/2 \rightarrow 3/2 \pm 1/2$	20.80	24.2 ± 3.9
$1/2 \pm 1/2 \rightarrow 3/2 \mp 1/2$	27.35	31.5 ± 3.9
$3/2 \pm 3/2 \rightarrow 1/2 \pm 1/2$	15.06	15.8 ± 1.3
$3/2 \mp 3/2 \rightarrow 1/2 \pm 1/2$	35.81	35.4 ± 2.3
$3/2 \pm 3/2 \rightarrow 3/2 \pm 1/2$	27.94	28.3 ± 2.4
$3/2 \pm 3/2 \rightarrow 3/2 \mp 1/2$	21.14	24.3 ± 2.1
$3/2 \pm 3/2 \rightarrow 3/2 \mp 3/2$	3.63	5.6 ± 0.6
$3/2 \pm 1/2 \rightarrow 3/2 \mp 1/2$	12.69	10.8 ± 4.3

Table II illustrates the accuracy of the present quantum-mechanical calcu-

lations using PP adiabatic potential energies. Except for the 3/2 $\pm$ 3/2 $\rightarrow$ 3/2 $\mp$ 3/2 transition, all the calculated thermal averaged cross-sections for Zeeman transitions are in excellent agreement with the measurement of Gay and Schneider (1976).

Figure 16 shows comparisons of our results with experiment and previous calculations for the disorientation cross section $\sigma^{(1)}_{1/2} = 2\,\overline{\sigma}$ (1/2 1/2 $\rightarrow$ 1/2 -1/2) for Rb ($5^2P_{1/2}$) + He collisions. Our calculations using the PP adiabatic potential energies improve much the calculations of Brouillaud and Gayet (1977) and those of Doebler and Kamke (1977) using liPP adiabatic potential energies. Our results are in excellent agreement with the measu-

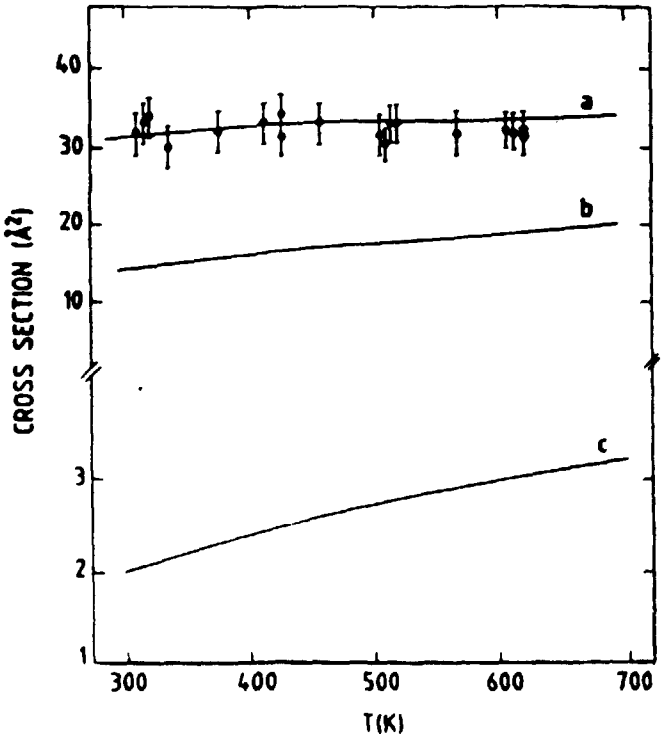

Fig. 16 - Disorientation cross-section $\sigma^{(1)}_{1/2} = 2\,\overline{\sigma}$ (1/2 1/2 $\rightarrow$ 1/2 -1/2) for Rb (5^2P) + He collisions, versus temperature. Theory : a) thermal averaged cross sections obtained from PP potential curves (Pascale, 1983 a,b) ; calculations of Brouillaud and Gayet using liPP potential curves (Baylis, 1969) ; calculations of Doebler and Kambe (1979) using liPP potential curves (Pascale and Vandeplanque, 1974). The experimental data, with error bars, are those of Doebler and Kamke (1979).

rements of Doebler and Kamke (1977). The improvement of the PP calculations over previous calculations using liPP adiabatic potential energies is clearly seen also in the comparison of the calculated energy-dependence of the cross sections for fine-structure transitions with crossed-beam experimental data (see Figs. 17 and 18). Figure 17 shows the very good agreement which is observed between experiment (Mestdagh, 1982 ; Mestdagh

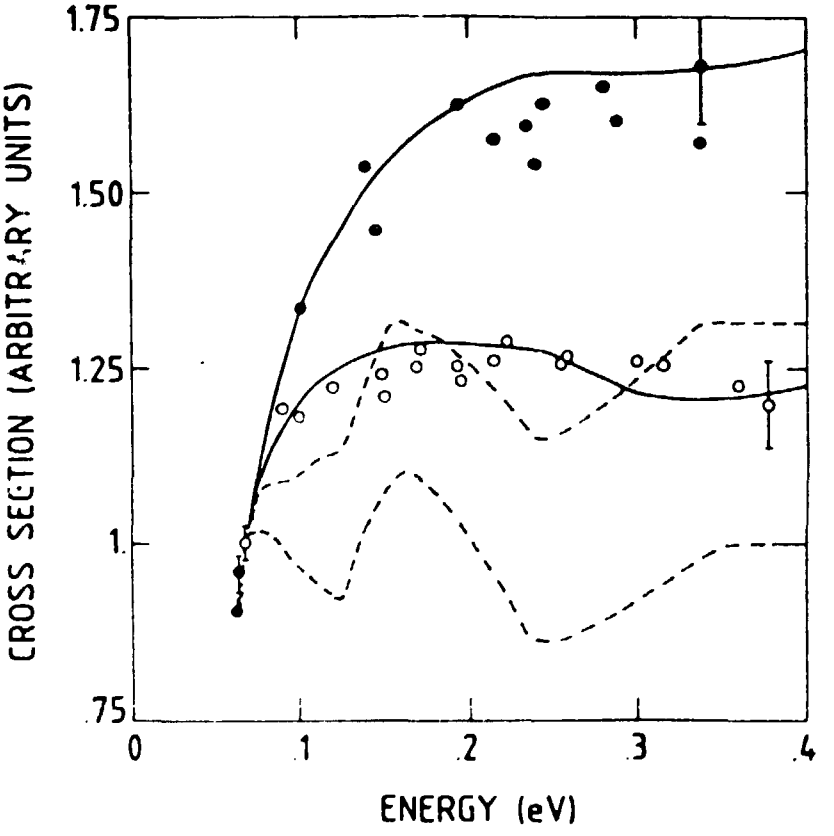

Fig. 17 - Energy-dependence of the $4^2P_{3/2} \rightarrow 4^2P_{1/2}$ transition cross section for K (4^2P) + He collisions. Experiment (Mestdagh et al., 1982) : full circle, unpolarized excitation of the $4^2P_{3/2}$: open circle, circularly polarized excitation of K from the $4S_{1/2}$ F = 2 level to the $4P_{3/2}$ F = 3 level. Theory : dashed line, calculations of Pascale and Perrin (1980) using liPP potential curves (Pascale and Vandeplanque, 1974) ; full line, present results using PP potential curves.

et al., 1982) and theory (when PP adiabatic potential energies are used) concerning polarization effects in the $4^2P_{3/2} \rightarrow 4^2P_{1/2}$ transition in collisions of K with He. We recall that here, polarization effects result from

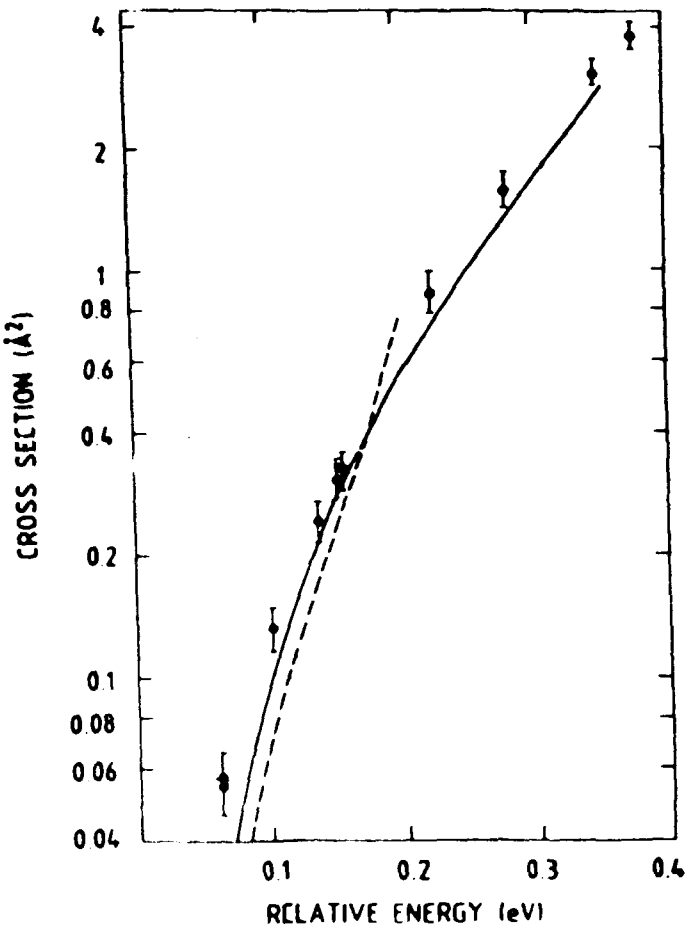

Fig. 18 - Energy dependence of the $5^2P_{1/2} \rightarrow 5^2P_{1/2}$ transition cross section for $Rb(5^2P)$ + He collisions. Theory : full line, present results using PP potential curves ; dashed line, calculations of Olson (1975) using liPP potential curves (Baylis, 1969). The crossed-beam experimental data Mestdagh, 1982), shown with error bars, were normalized to cell measurements (Gallagher, 1968).

the very different energy-dependence of the Zeeman cross sections (Pascale and Perrin, 1980). Figure 18 shows comparisons between crossed-beam experimental data (see, Mestdagh, 1982) and quantum mechanical calculations of the $5^2P_{1/2} \rightarrow 5^2P_{3/2}$ transition cross section in $Rb(5^2P)$ + He collisions. Agreement between experiment and theory (using PP adiabatic potential energy) is seen to be very good both for the absolute values of the cross section, and its energy dependence.

A.3 - Second and third n^2P levels of Rb and Cs. In this case the terms

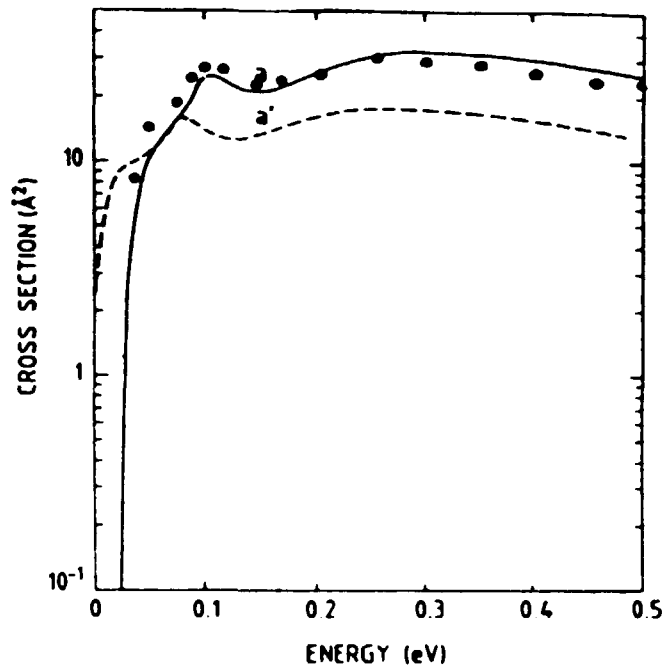

Fig. 19 - Present quantum-mechanical cross section calculations for the $7^2P_{1/2} \rightarrow 7^2P_{3/2}$ (full line) and $7^2P_{3/2} \rightarrow 7^2P_{3/2}$ (dashed line) transitions in Cs (7^2P) + He collisions. The full circles are the results of a four $\Omega = 1/2$ channel quantum-mechanical calculation using PP diabatic potential energies and radial coupling (Pascale and Kimura, 1985).

$\tilde{v}_{0,2}(R)$ have been calculated following the method defined above. Because the $\tilde{v}_2(R)$ terms may show several maxima, oscillation in the energy dependence of the total cross sections is generally observed. For example, Figure 19 shows the energy-dependence of the $7P_{1/2} \rightleftarrows 7P_{3/2}$ transition cross sections calculated by the quantum-mechanical method developed above and the results of a four $\Omega = 1/2$ channel quantum-mechanical calculation using the diabatic picture (Pascale and Kimura, 1985). In this latter calculation, radial coupling between the four $\Omega = 1/2$ molecular states emerging from the $7^2P_{1/2}$ and $3/2$ and $6^2D_{3/2}$ and $5/2$ levels (see Fig. 20) have been calculated ; then, by a unitary transformation the coupled equation set for the scattering problem formulated in the body-fixed frame was transformed from the adiabatic picture to the diabatic picture, and the cross-sections were calculated. Comparison between the two calculations show a good overall agreement ; this indicates that radial coupling is mainly

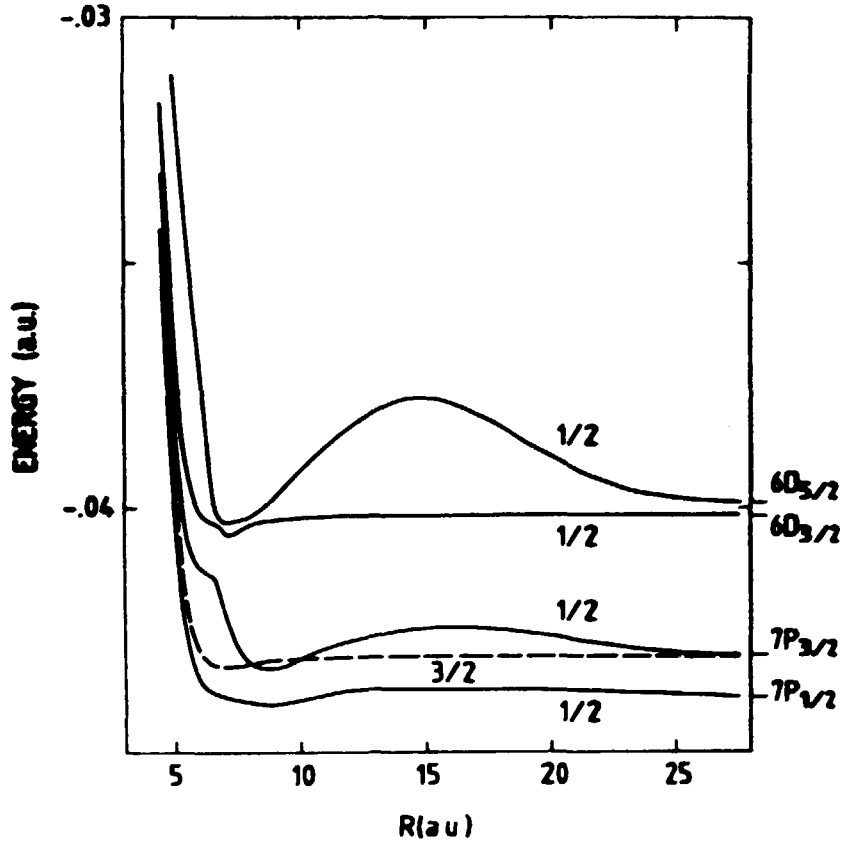

Fig. 20 - Ω = 1/2-PP adiabatic potential energies of the CsHe system, correlated asymptotically to the 7^2P and 6^2D levels of Cs.

responsible for the fine-structure transition and that, moreover, coupling with neighbouring states does not affect the calculation of the cross sections, in the present case. The thermally averaged cross sections calculated for the $7^2P_{3/2} \rightarrow 7^2P_{1/2}$ transition are seen in good agreement with experimental data in Table III. In the case of the $n^2P_{3/2} \rightarrow n^2P_{1/2}$ transitions in Rb (with n = 6, 7) experiment and theory are also found in very good agreement (Pascale, 1983c). In the case of the $8^2P_{1/2} \rightarrow 8^2P_{3/2}$ transition in Cs, the PP quantum-mechanical calculations (Pascale, 1983c) give a substantial improvement over previous IiPP semiclassical calculations (Pascale and Stone, 1976), but comparison with experimental data indicates that coupling with the 7^2D level cannot be ignored in that case. Finally, Table IV shows very good agreement between the present results and the recent measurements of Lukaszewski and Jackowska (1984)

Table III - Thermally averaged cross-sections in $\mathring{A}^2$ for the $7^2P_{3/2} \rightarrow 7^2P_{1/2}$ transition in Cs, induced in collisions with He.

T (K)	Present results	Experiment (a)	(b)	(c)
320	11.0 (12.6)*			12.8 ± 2.6
405	11.7 (13.5)	15.2 ± 4.6		
450	12.2 (13.7)		11.0 ± 2.0	
520	12.5 (14.2)	14.9 ± 4.5		
615	13.0 (14.4)		11.0 ± 2.0	
630	13.1 (14.5)		15.6 ± 4.7	

(a) Siara et al. (1974).
(b) Cuvellier et al. (1975).
(c) Munster and Marek (1981).
* four 1/2-channel quantum-mechanical calculation (see text).

Table IV - Thermally averaged cross-sections for depolarization in the second $n^2P_{3/2}$ level of Rb and Cs (in 10^{-14} cm^2) for T = 340 K.

	Theory present	Experiment (a)	(b)	(c)	(d)
Rb($6^2P_{3/2}$)	5.11	4.56 (21)	4.3		
Cs($7^2P_{3/2}$)	5.62	4.99 (16)		7.2	7.2

(a) Lukaszewski and Jackowska (1983).
(b) Grosswendt (1969).
(c) Minemoto et al. (1974).
(d) Minemoto and Kakihara (1976).

for depolarization in the second $n^2P_{3/2}$ level of Rb and Cs.

B - Excitation from the ground-state to the first n^2P level of an M-atom in collisions with He, in the keV energy range.

In the following, we consider the process

$$M(n^2S) + He \rightarrow M(n^2P) + He \qquad (52)$$

in which an M-atom is excited from the ground state n^2S to the first excited n^2P level in collisions with He. Collisional excitation of an M-atom by rare gases (mainly He and Ne) have been the subject of several investigations, both theoretical and experimental (see, for example, the review article by Andersen and Nielsen, 1982). Two different mechanisms have been proposed for the excitation process : i) for $E < 1$ keV, where E is the collision energy of the system, the excitation process proceeds through a molecular crossing mechanism involving excited states of the rare gas atom (Courbin-Gaussorgues et al., 1979) ; for $E \gtrsim 1$ keV the excitation process results from a direct mechanism involving only the M-atom valence electron (Manique et al., 1977 ; Nielsen et al., 1978). For treating the one-electron mechanism, a semiclassical approach was used, in which the wave-function of the system was represented by a linear combination of atomic orbitals : liPP or MP interactions were used, as well as frozen-core Hartree-Fock interactions. More recently, we have investigated Reaction (52) using a multichannel perturbed-stationary-state (PSS) approach and the PP molecular-structure calculations (Pascale, 1983a).

B.1 - Theory. In the multichannel PSS approach, one has to solve the time-dependent Schrödinger equation,

$$i \frac{\partial}{\partial t} \psi = H_{eff} \psi \qquad (53)$$

where H_{eff} is the one-electron effective Hamiltonian used in the PP molecular-structure calculation approach (see Eqs. (7) and (8)) and its t-dependence arises through R(t). The scattering wave function ψ is expanded in terms of Born-Oppenheimer (BO) wave functions,

$$\psi = \sum_i a_i(t)\ \phi_i^{BO}\ (\vec{r},R)\ F_i \tag{54}$$

where

$$H_{eff}\ \phi_i^{BO}\ (\vec{r},R) = E_i(R)\ \phi_i^{BO}\ (\vec{r},R) \tag{55}$$

and $E_i(R)$ is the PP adiabatic potential energy for molecular state i. In Eq. (54), F_i is an electronic translation factor (ETF) (see, Kimura and Thorson, 1981) which can be expanded in terms of the relative velocity $\vec{v}$ of the system, and in terms of f_i, a state-dependent switching function for representing, during the collision, a local propagation of the electron velocity in the quasimolecule. Then, to the first order in $\vec{v}$, the following coupled equations results from Eqs. (53)-(54) :

$$\dot{a}_j = -\,i\,E_i\,a_j + \sum_i \vec{v}\ .\ (\vec{P} + \vec{A})_{ji}\ a_i \tag{56}$$

in which

$$\vec{P}_{ji} = \langle j \mid -i\,\vec{\nabla}_R \mid i\rangle \tag{57}$$

is the non adiabatic coupling, and $\vec{A}_{ji}$ is an ETF correction to the coupling,

$$\vec{A}_{ji} = -\,i\,\langle j \mid \frac{1}{2}\,f_i\,\vec{\nabla}_r \mid i\rangle\ . \tag{58}$$

In the present calculations, because the BO wave functions are expanded over one-center basis functions only, the ETF's are unimportant, but they are crucial in the case of a rearrangement process (see, for example, Kimura et al., 1982). In a rotating coordinate frame (or body-fixed frame), one may separate the coupling term in Eq. (56) into a radial coupling term and a rotational coupling term,

$$\vec{v}\ .\ (\vec{P} + \vec{A}) = \dot{R}\ (P + A)^R + \dot{\theta}\ (P + A)^\theta\ , \tag{59}$$

in which ETF corrections to the usual radial and rotational coupling terms arise. In our approach, a straight-line trajectory has been assumed for describing the relative motion of the system, so that

$$\dot{R} = \frac{v_o}{R}\,z \tag{60}$$

and

$$\dot{\theta} = \frac{b\, v_o}{R^2} \tag{61}$$

where v_o is the initial relative velocity of the system, and b the impact parameter. Recalling that the BO wave function is expanded in terms of STO's centered on the M-ion (center A), for which the non-linear parameters where optimized at $R \to \infty$ (so that no R-dependence arises in the STO's),

$$\phi_i^{BO}(\vec{r},R) = \sum_\alpha C_{i\alpha}^A(R)\, \varphi_\alpha^A(\vec{r}) \quad , \tag{62}$$

the coupling matrix elements can be easily calculated :

$$(P + A)_{ji}^R = - i \sum_\alpha \sum_\beta C_{j\beta}^A \frac{d}{dR} C_{i\alpha}^A(R) \langle \varphi_\beta^A | \varphi_\alpha^A \rangle \tag{63}$$

and

$$(P + A)_{ji}^\theta = - i \sum_\alpha \sum_\beta C_{j\beta}^A(R)\, C_{i\alpha}^A(R) \langle \varphi_\beta^A | i l_y | \varphi_\alpha^A \rangle \tag{64}$$

where l_y is the component of the orbital angular momentum along the axis perpendicular to the collision plane. The coupled equation set (Eq. (56)) is then integrated numerically, for an initial relative velocity v_o and impact parameter b, with the usual initial conditions :

$$a_j(-\infty) = \delta_{ij} \ , \tag{65}$$

where i denotes the initial channel, and the probability for the $i \to j$ transition is :

$$P_{ij}(v_o,b) = | a_j(+\infty ; v_o, b) |^2 \tag{66}$$

Finally, the total cross section for the $i \to j$ transition is :

$$Q_{i \to j}(v_o) = 2\pi \int_0^\infty P_{i \to j}(v_o,b)\, b\, db \tag{67}$$

B.2 - Calculations and results. The multichannel-PSS calculations were performed with a molecular basis set including the first five Σ states and the first three Π states. Radial and rotational coupling terms between all

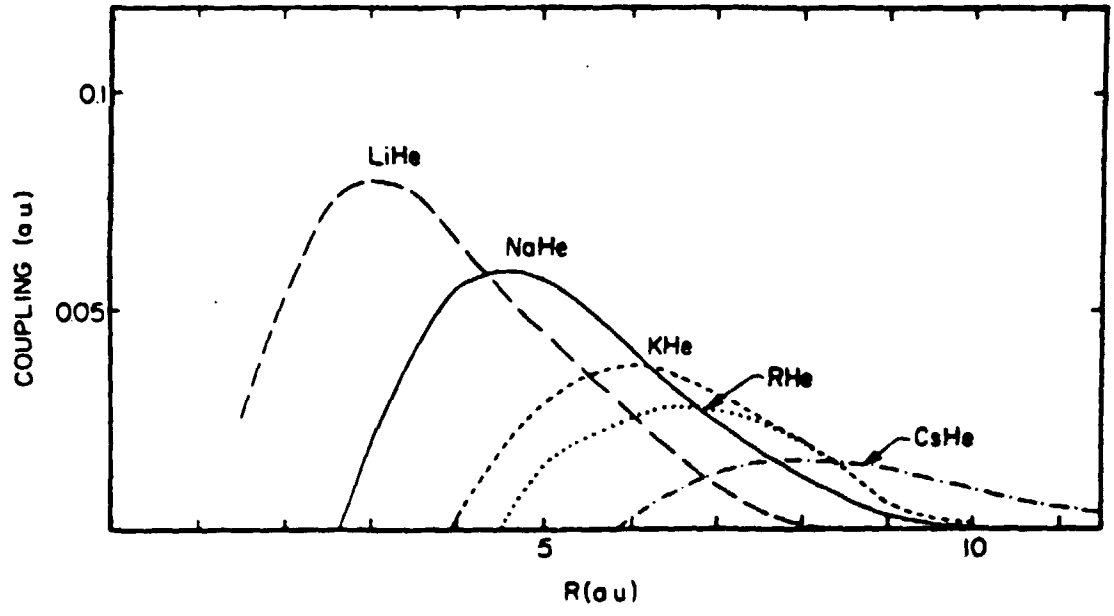

Fig. 21 - Radial coupling between 1Σ and 2Σ molecular states of the M-atom-He systems, as indicated in the figure.

the states were calculated. Figure 21 shows the broad peak of the 1Σ-2Σ radial coupling, which was found the most important radial coupling for these calculations, for all the M-atom-He systems. The position of this peak shifts towards larger R, and its magnitude decreases, as the M-atom changes from Li to Cs. The 1Σ-1Π rotational coupling was also found the most important rotational coupling for these calculations ; it also presents a broad peak which behaves as the 1Σ-2Σ radial coupling when the M-atom changes. However, the decrease of coupling when one goes from Li to Cs will be compensated more or less by the decrease in the energy differences of the molecular states. Radial and rotational coupling between other states involved in the calculations present different characteristics depending on the M-atom ; they may contribute more or less significantly to the collision process, depending upon the collision energy. For example, we have reported in Figs. 22 and 23 the product $P_{i\to j} \times b$, versus b, for excitation from de 1Σ state, i, to excited channel j in Rb(5S) + He collisions, for center of mass energy E_{CM} = 0.5 keV and E_{CM} = 4 keV, respectively. At E_{CM} = 0.5 keV, the dominant channel is found to be the $5p\sigma$ state, resulting from the 1Σ-2Σ radial coupling. At E_{CM} = 4 keV, the $5p\pi$ state

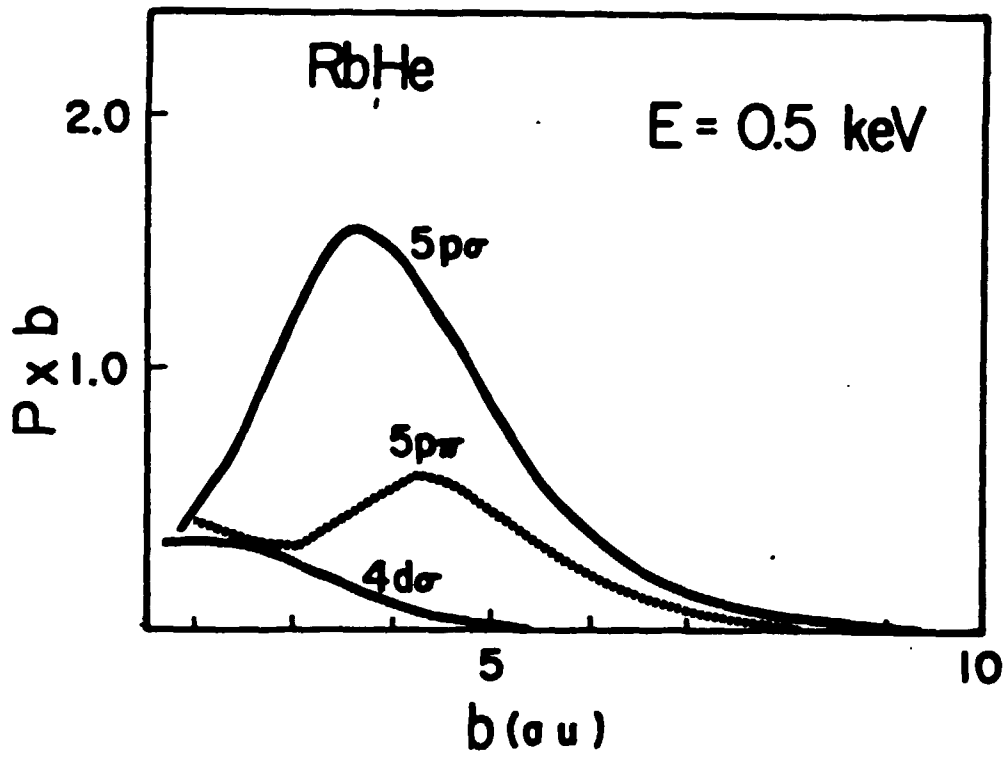

Fig. 22 - Transition probability times the impact parameter b, versus b, for excitation from the 1Σ ($5s\sigma$) to the 2Σ ($5p\sigma$), 3Σ ($4d\sigma$) and 1Π ($5p\pi$) states of Rb He system (as indicated in the figure) at center of mass energy E = 0.5 keV.

becomes the dominant channel for the 5S → 5P excitation in Rb, because of the 1Σ-1Π rotational coupling ; but, also the $4d\sigma$ excitation probability becomes comparable with that of the $5p\sigma$ excitation (resulting not from a direct excitation through the 1Σ-3Σ radial coupling, but by 1Σ-1Π rotational coupling followed by 1Π-3Σ rotational coupling). The cross sections for excitation of the M-atoms in collisions with He, from the ground-state to the first n^2P level, are shown in Fig. 24, over large range of laboratory energies (note that He is the target). All the cross sections present a broad main peak ; its position shifts towards higher energies when the M-atom changes from Li to Cs and its magnitude decreases in agreement with the behavior of the main rotational and radial coupling and the energy differences discussed above. The position of this main peak is closely related to the Massey parameter $\lambda_M = \frac{\Delta E\, a}{\hbar v}$ (as discussed, for example, by

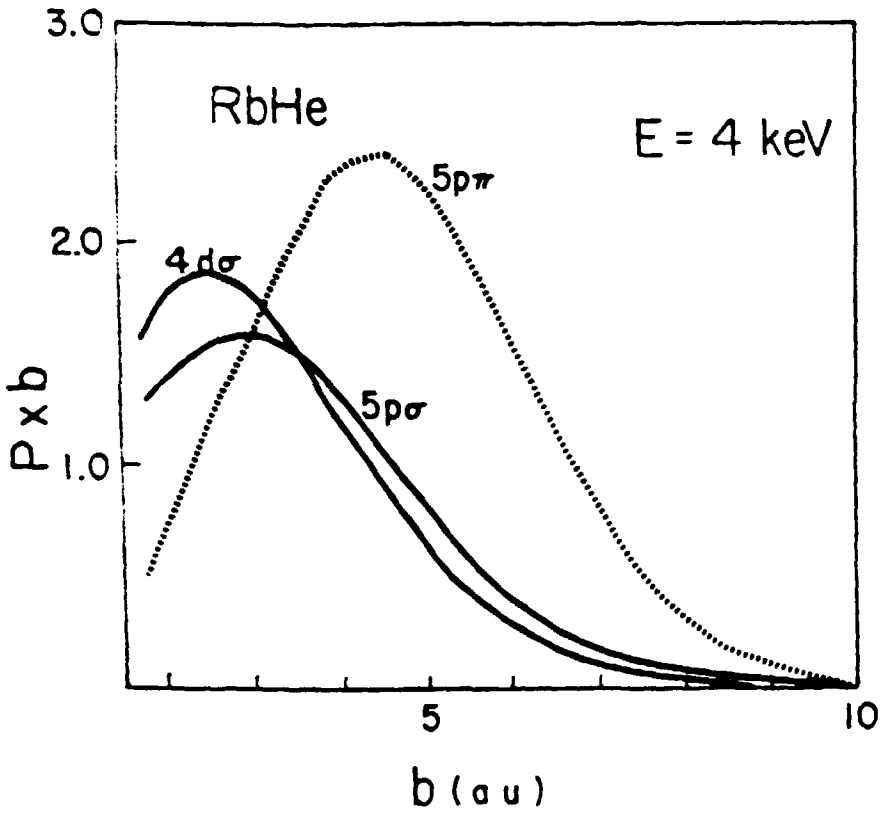

Fig. 23 - Same as Fig. 22 except at E = 4 keV.

Andersen et al., 1979), in which ΔE is the threshold of the n^2S-n^2P transition, v is the relative velocity corresponding to the energy at the peak, and α is an effective range of the interaction. If α is defined, for example, by the position of the maximum in the main radial coupling (see Fig. 21) one finds that λ_M is nearly constant : λ_M = 1.91, 2.15, 2.11, 2.22 and 1.90, respectively, for Li, Na, K, Rb and Cs. The origin of the shoulder observed in the cross sections at lower energies (see Fig. 24) is unclear. However, the structure in the cross sections may be attributed to increassing contribution of the main rotational coupling for the heavier M-atom-He systems, as discussed above, when the energy increases.

Finally, Figures 25 and 26 show comparison between the present results and experimental data for the Na(3S) + He and K(4S) + He collisions, respecti-

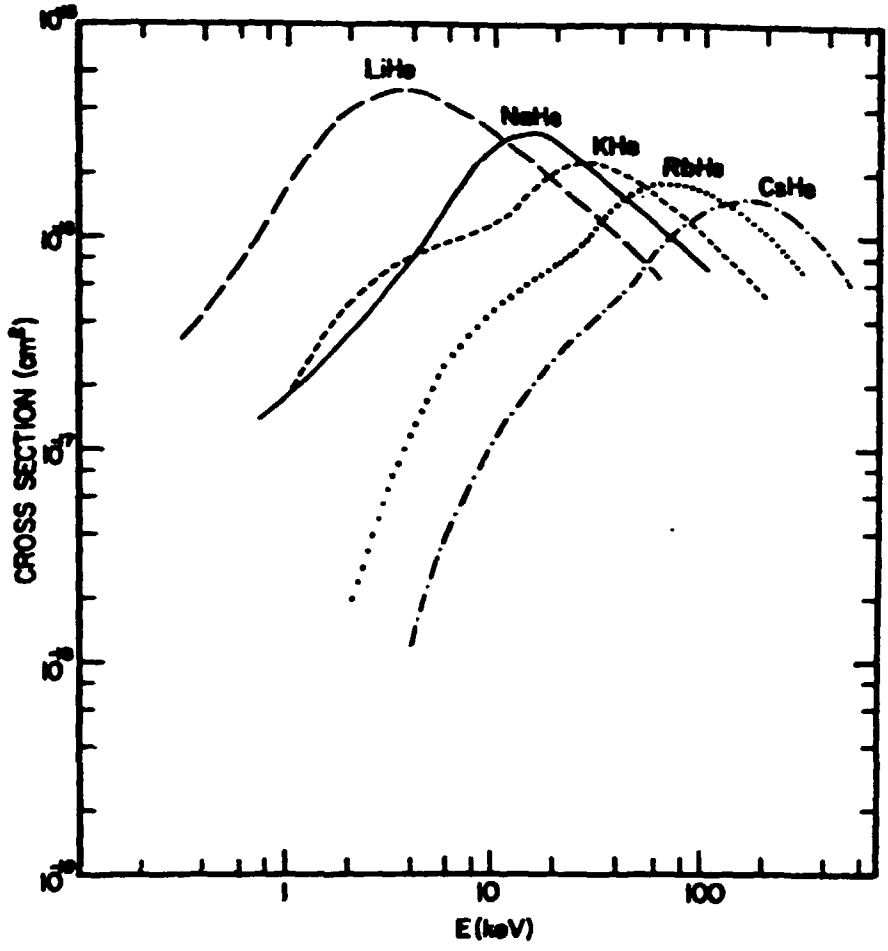

Fig. 24 - Cross-sections for excitation of the M-atom from the ground-state to the first n^2P level, in M-atom-He collisions as indicated in the figure, versus the laboratory energy E.

vely. Agreement between experiment and theory is quite good, both for the position and the absolute value of the main peak in the cross sections. For the Na(3S) + He collision, our multichannel PSS calculations using the PP adiabatic potential energies and molecular wave function above reported, improve significantly, at lower energies, the agreement between experiment and previous calculations based on an atomic orbital expansion and using 1iPP or HF frozen core interactions. The same observations were made in the case of the Li(2S) + He collision (Kimura and Pascale, 1985).

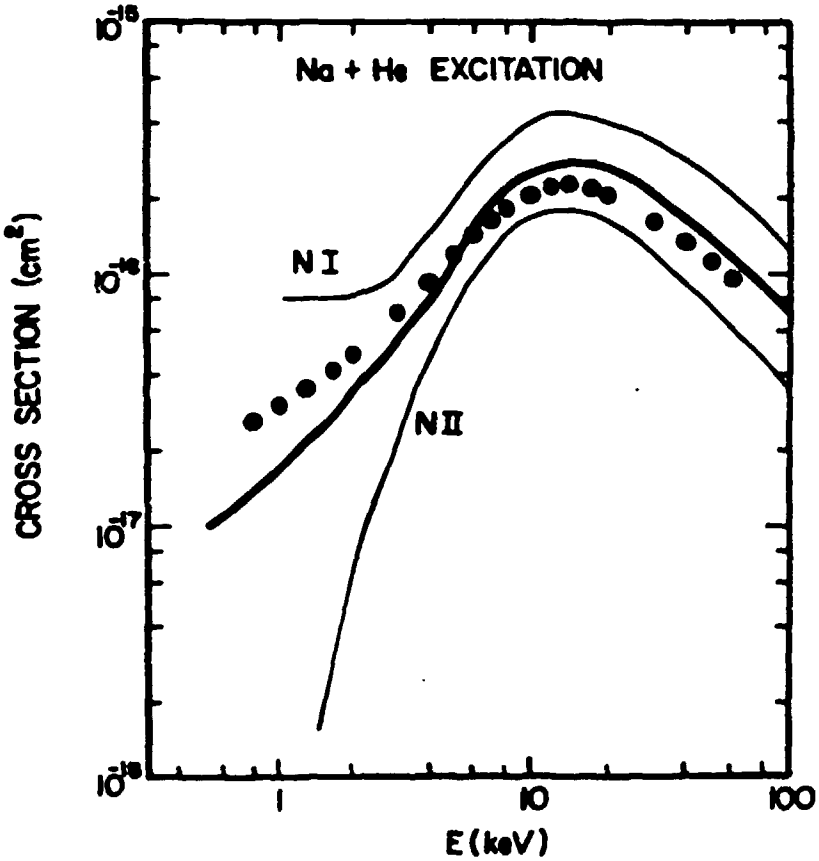

Fig. 25 - 3p excitation cross sections for Na(3S) + He collisions, versus the laboratory energy E. Heavy full curve, present results ; NI, Manique et al. (1977) calculation using liPP interaction (Baylis, 1969) : NII, Manique et al. (1977) calculation using an HF frozen core potential ; full circles, experimental data (Nielsen et al., 1978).

For the K + He collision, our calculations are only in qualitative agreement with the experimental data for the structure observed in the cross-section, at lower energies.

This overall agreement between experimental data and the present results, confirms the reliability of the PP approach for determining quite realistic adiabatic potential energies and wave functions, over a large domain of internuclear distances.

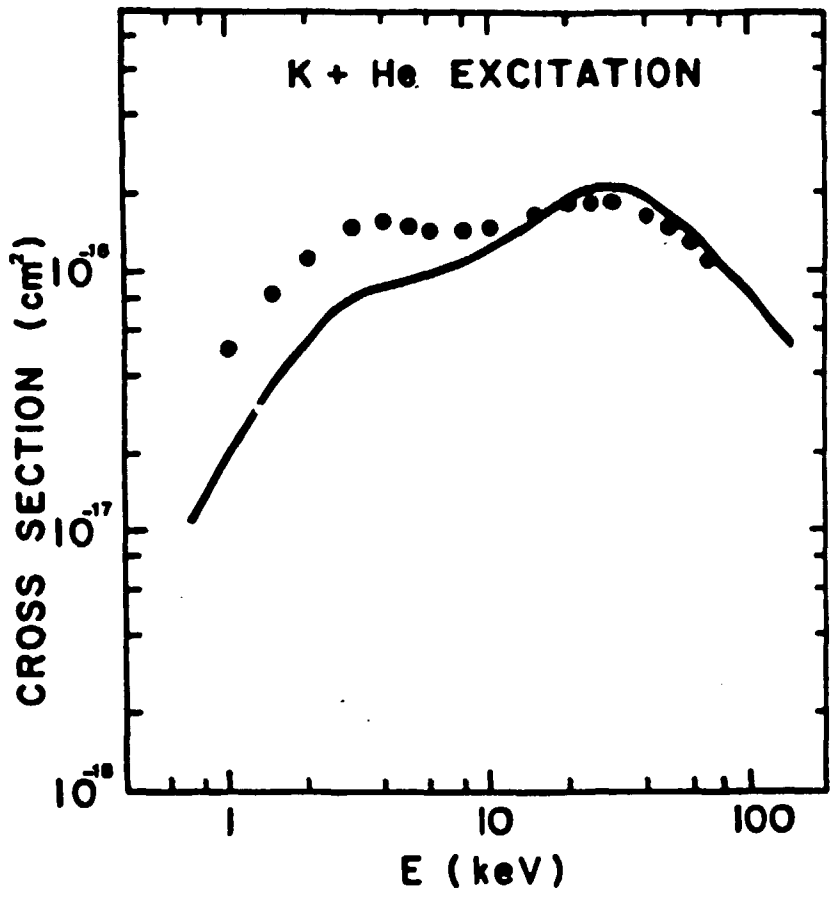

Fig. 26 - 4p excitation cross section for K(4S) + He collisions, versus the laboratory energy E. Full curve, present results ; full circles, experimental data (Andersen et al., 1979).

4. Conclusion

We expect to have shown, from specific but we think quite representative examples, that the use of semiempirical effective interactions (and more particularly, the PP approach) is a quite powerful method for molecular-structure calculations and a detailed study of various collision problems. When the semiempirical effective interactions are carefully determined, their use in molecular-structure calculations or collision problems can lead to quite realistic predictions, which generally compare favorably with experimental data.

In the MP approach, one generally defines a local interaction and one constraints the valence electron wave function to be orthogonal to all the core orbitals. In the PP approach, a semi-local interaction is defined (in the sense that it is l-dependent) so that the Pauli principle is implicitely satisfied. But, while the two approaches should give very close results, in principle (at least for the one-electron systems), the PP approach offers an undeniable advantage over the MP approach ; it is to have not to consider the core orbitals. This allows us to reduce considerably the basis set in molecular-structure calculations (it is even limited to a one-center expansion for some systems) and to treat systems with a large number of electrons. Moreover, for systems with more than one-valence electron, instabilities may arise in MP calculations due to mixing with an indefinite number of virtual states. Nevertheless, both MP and PP approaches have been used successfully in recent years for various one-electron systems. Work is now in progress in various laboratories to apply these methods to systems with two valence electrons (alkali-earth-rare gas, alkali-alkali interactions for example). However, more improvements in the methods should be made in the future : in particular, to obtain a better knowledge of the cross-term everywhere or a better determination of the core-core interaction. Such improvements in semiempirical effective interaction methods should allow one to provide in the future useful information for systems for which *ab initio* approaches are manageable with difficulty. For treatment of reactive collision problems, *ab initio* methods are particularly very difficult to use for calculations of non-adiabatic coupling. Therefore, extension of the PP approach to more than two-center systems may be very useful and should be envisaged in the future.

Acknowledgments

I would like to thank Prof. W.E. Baylis and Dr. F. Rossi for many stimulating and fruitful discussions during the preparation of this paper. I would like to acknowledge also contributions of Prof. R.E. Olson, Drs. M. Kimura and F. Rossi to the work presented here.

References

. Ahmad-Bitar R., Lapatovich R., Pritchard D.E., and Renhorn I. : Phys. Rev. Lett. 39, 1657 (1977).

. Alfaro V. de, and Regge T. : in Potential Scattering, p. 44 (North-Holland Publishing Company, Amsterdam 1965).

. Andersen N., Andersen T., Hedegaard P., and Olsen J.O. : J. Phys. B 12, 3713 (1979).

. Andersen N., and Nielsen S.E. : Adv. At. Mol. Phys. 18, 265 (1982).

. Arthurs A.M., and Dalgarno A. : Proc. R. Soc. A 256, 540 (1960).

. Balling L.C., Wright J.J., and Havey M.D. : Phys. Rev. A 26, 1426 (1982).

. Bardsley J.N. : Case Stud. At. Phys. 4, 299 (1974).

. Barthelat J.C., Durand Ph., and Seraphini A. : Mol. Phys. 33, 159 (1977).

. Baylis W.E. : J. Chem. Phys. 51, 2665 (1969).

. Baylis W.E. : in Progress in Atomic Spectroscopy, ed. Hanle W. and Kleinpoppen H., Part B, Chap. 28 (Plenum Press, 1979).

. Botschwina P., Meyer W., Hertel I.V., and Reiland W. : J. Chem. Phys. 75, 5438 (1981).

. Bottcher C., and Dalgarno A. : Proc. R. Soc. A 340, 187 (1974).

. Brouillaud B. and Gayet R. : J. Phys. B 10, 2143 (1977).

. Buckingham A.C. : Adv. Chem. Phys. 12, 107 (1967).

. Chang E.S. : J. Phys. B 14, 893 (1981).

. Courbin-Gaussorgues C., Wahnon P., and Barat M. : J. Phys. B 12, 3047 (1979).

. Cuvellier J., Fournier P.R., Gounand F., Pascale J., and Berlande J. : Phys. Rev. A 11, 846 (1975).

. Czuchaj E. : Z. Physik A 292, 109 (1979).

. Czuchaj E., and Sienkiewicz J. : Z. Naturforsch A 34, 694 (1979).

. Czuchaj E., and Sienkiewicz J. : J. Phys. B 17, 2251 (1984).

. Czuchaj E., and Sienkiewicz J. : Z. Naturforsch (1985), to appear.

. Dixon R.N., and Robertson I.L. : Mol. Phys. 36, 1099 (1978).

. Doebler H., and Kamke B. : Z. Phys. A 280, 111 (1977).

. Ferray M., Visticot J.P., Lozingot J., and Sayer B. : J. Phys. B 13, 2571 (1980).

. Gadea X.F., Jeung G.H., Pelissier M., and Malrieu J-P., Picqué J.L., Rahmat G., Verges J., and Vetter R. : Laser Chem. 2, 361 (1983).

. Gallagher A. : Phys. Rev. A 172, 88 (1968).

. Gay J-C., and Schneider W.B. : Z. Phys. A 278, 211 (1976).

. Grosswendt B. : Z. Naturforsch 24a, 1424 (1969).

. Hanssen J., Mc Carroll R., Valiron P. : J. Phys. B 12, 899 (1979).

. Hara S. : J. Phys. Soc. Jpn. 22, 710 (1967).

. Havey M.D., Frolking S.E., and Wright J.J. : Phys. Rev. Lett. 45, 1783 (1982).

. Hliva M., Barthelat J.C., and Malrieu J.P. : J. Phys. B 18, 2433 (1985).

. Inouye H., Noda K., and Kita S. : J. Chem. Phys. 71, 2136 (1979) ; and references therein.

. Kahn L.R., Baybutt P., and Truhlar D.G. : J. Chem. Phys. 65, 3826 (1976).

. Karl G., Poll J.D. : J. Chem. Phys. 46, 2944 (1967).

. Kimura M., Olson R.E., and Pascale J. : Phys. Rev. A 26, 3113 (1982).

. Kimura M., and Pascale J. : J. Phys. B 18, 2719 (1985).

. Kimura M., and Thorson W.R. : Phys. Rev. A 24, 1780 (1981).

. Kolos W., and Wolniewicz L. : J. Chem. Phys. 46, 1426 (1967).

. Krauss M. : J. Res. Natl. Bur. Stand., A72, 553 (1968).

. Krauss M., Maldonado P., and Wahl C. : J. Chem. Phys. 54, 4944 (1971).

. Lakowski B.C., Langhoff S.R., and Stallcop J.R. : J. Chem. Phys. 75, 815 (1981).

. Linder F., and Schmidt H. : Z. Naturforsch. A26, 1603 (1971).

. Lukaszewski M., and Jackowska I. : Opt. Commun. 46, 89 (1983).

. Manique J., Nielsen S.E., and Dahler J.S. : J. Phys. B 10, 1703 (1977).

. Masnou-Seeuws F. : J. Phys. B 15, 883 (1982).

. Masnou-Seeuws F., Philippe M., and Valiron P. : Phys. Rev. Lett. 41, 395 (1978).

. Mason C.R., and Peach G. : in Spectral Line Shapes, ed. F. Rostas, Chap. 3, p. 643 (de Gruyter, 1985).

. Mestdagh J.M. : Thèse, Université de Paris-Nord (1982).

. Mestdagh J.M., Berlande J., de Pujo P., Cuvellier J., and Binet A. : Z. Phys. A 304, 3 (1982).

. Mies F.H. : Phys. Rev. A 7, 942 (1973).

. Minemoto T., Goto T., and Kanda T. : J. Phys. Soc. Jpn. 36, 918 (1974).

. Minemoto T., and Kakihara K. : J. Phys. Soc. Jpn. 41, 984 (1976).

. Mó O., Riera A., and Yáñez M. : Phys. Rev. A 31, 3977 (1985).

. Munster P., and Marek J. : J. Phys. B 14, 1009 (1981).

. Nielsen S.E., Andersen N., Andersen T., Olsen J.O., and Dahler J.S. : J. Phys. B 11, 3187 (1978).

. Nikitin E.E. : Adv. Chem. Phys. 28, 317 (1975).

. O'Callagham M., Holstein T., and Gallagher A. (1985): to be published.

. Olson R.E. : Chem. Phys. Lett. 33, 250 (1975).

. O'Malley T.F., Burke P.G., and Berrington K.A. : J. Phys. B 12, 953 (1979).

. Pascale J. : J. Chem. Phys. 67, 204 (1977).

. Pascale J. : Phys. Rev. A 28, 632 (1983a).

. Pascale J. : 13th ICPEAC Berlin (Ed. Eichler J. et al.), 313 (1983b) ; ib., 342 (1983c) ; to be published.

. Pascale J. : in Spectral Line Shape, ed. F. Rostas, Chap. 3, 563-586 (de Gruyter, 1985) ; and references therein.

. Pascale J., and Kimura M. (1985), to be published.

. Pascale J., Mestdagh J.M., Cuvellier J., and de Pujo P. : J. Phys. B 17, 2627 (1984).

. Pascale J., and Perrin M-Y. : J. Phys. B 13, 1839 (1980).

. Pascale J., and Stone P.M. : J. Chem. Phys. 65, 5122 (1976).

. Pascale J., and Vandeplanque J. : J. Chem. Phys. 60, 2278 (1974).

. Peach G. : Comments At. Mol. Phys. 11, 101 (1982).

. Peach G. : in Atoms in Astrophysics, ed. Burke P.G. et al., Chap. 5 (Plenum, 1983).

. Philippe M., Masnou-Seeuws F., and Valiron P. : J. Phys. B 12, 2493 (1979).

. Reid R.H.G. : J. Phys. B 6, 2018 (1973).

. Rossi F., and Pascale J. : Phys. Rev. A 32, 2657 (1985).

. Saxon R., Olson R.E., and Liu B. : J. Chem. Phys. 27, 2692 (1977).

. Siara I.N., Kwong H.S., and Krause L. : Can. J. Phys. 52, 945 (1974).

. Slater J.C., and Kirkwood J.G. : Phys. Rev. A 37, 682 (1931).

. Szudy J., and Baylis W.E. : J. Quant. Spectrosc. Radiat. Transfer 15, 641 (1975).

. Visticot J.P., Pascale J., and Sayer B. : J. Phys. B 18, 2861 (1985).

. Wagner A.F., Wahl A.C., Karo A.M., and Krejci R. : J. Chem. Phys. 69, 3756 (1978).

. Weeks J.D., Hazi A., and Rice S.A. : Adv. Chem. Phys. 16, 283 (1969).

. Williams J.F. : J. Phys. B 12, 265 (1979).

. York G., Scheps R., and Gallagher A. : J. Chem. Phys. 63, 1052 (1975).